Trypanosomal variant surface glycoprotein expression in human African trypanosomiasis patients

Jaime So[1**], Sarah Sudlow[1**], Abeer Sayeed[1], Tanner Grudda[1], Stijn Deborggraeve[2#], Dieudonné Mumba Ngoyi[3], Didier Kashiama Desamber[4], Bill Wickstead[5], Veerle Lejon[6], and Monica R. Mugnier[1*]

[1]Department of Molecular Microbiology and Immunology, Johns Hopkins Bloomberg School of Public Health, Baltimore, Maryland, United States of America

[2]Department of Biomedical Sciences, Institute of Tropical Medicine, Antwerp, Belgium

[3]Department of Parasitology, Institut National de Recherche Biomédicale, Kinshasa, Democratic Republic of the Congo

[4]Programme Nationale de Lutte contre la Trypanosomiase Humaine Africaine, (PNLTHA), Ministry of Health, Kinshasa, Democratic Republic of the Congo

[5] School of Life Sciences, Queen's Medical Centre, University of Nottingham, Nottingham, NG7 2UH, United Kingdom

[6] UMR-177 Intertryp, Institut de Recherche pour le Développement, Centre de Coopération Internationale en Recherche Agronomique pour le Développement, University of Montpellier, Montpellier, France

**These authors contributed equally to the work
Current address: Médecins Sans Frontières - Access Campaign, Geneva, Switzerland

* Corresponding author
E-mail: mmugnie1@jhu.edu (MM)

Abstract

Trypanosoma brucei gambiense, an extracellular protozoan parasite, is the primary causative agent of human African trypanosomiasis. *T. b. gambiense* is endemic to West and Central Africa, where it is transmitted by the bite of infected tsetse flies. In the bloodstream of an infected host, the parasite evades antibody recognition by altering the Variant Surface Glycoprotein (VSG) that forms a dense coat on its cell surface through a process known as antigenic variation. Each VSG has a variable N-terminal domain exposed to the host and a less variable C-terminal domain that is partially hidden from host antibodies. Our lab developed VSG-seq, a targeted RNA-seq method, to study *VSG* gene expression in *T. brucei*. Studies using VSG-seq to characterize antigenic variation in a mouse model have revealed marked diversity in *VSG* expression within parasite populations, but this finding has not yet been validated in a natural human infection. Here, we used VSG-seq to analyze *VSGs* expressed in the blood of 12 patients infected with *T. b. gambiense*. The number of *VSGs* identified per patient ranged from one to 14; notably, two *VSGs* were shared by more than one patient. Analysis of expressed *VSG* N-terminal domain types revealed that 82% of expressed *VSGs* encoded a type B N-terminus, a bias not seen in datasets from other *T. brucei* subspecies. C-terminal types in *T. b. gambiense* infection were also restricted. These results demonstrate a bias either in the underlying *VSG* repertoire of *T. b. gambiense* or in this subspecies' expression of *VSGs* during infection. This work demonstrates the feasibility of using VSG-seq to study antigenic variation in human infections and highlights the importance of understanding *VSG* repertoires in the field.

Author Summary

Human African Trypanosomiasis is a neglected tropical disease primarily caused by the extracellular parasite *Trypanosoma brucei gambiense*. To avoid elimination by the host, these parasites repeatedly replace their dense surface coat of Variant Surface Glycoprotein (VSG). Despite the important role of VSGs in prolonging infection, *VSG* expression during natural human infections is poorly understood. A better understanding of natural *VSG* gene expression dynamics can clarify the mechanisms that *T. brucei* uses to alter its VSG coat and improve how trypanosomiasis is diagnosed in humans. We analyzed the expressed *VSGs* detected in the blood of patients with trypanosomiasis. Our findings indicate that parasites in both natural and experimental infections express diverse sets of *VSGs.*

Introduction

Human African Trypanosomiasis (HAT) is caused by the protozoan parasite *Trypanosoma brucei*. *T. brucei* and its vector, the tsetse fly, are endemic to sub-Saharan Africa [1]. There are two human-infective *T. brucei* subspecies: *T. b. gambiense,* which causes chronic infection in West and Central Africa (~98% of cases), and *T. b. rhodesiense,* which causes acute infection in East and Southern Africa (~2% of cases) [2,3]. In humans, infections progress from an early stage, usually marked by a fever and body aches, to a late stage associated with severe neurological symptoms that begins when the parasite crosses the blood-brain barrier [4]. HAT is considered fatal without timely diagnosis and treatment. While around 50 million people are at risk of infection [5], the number of annual human infections has declined significantly in recent years, with only 864 cases reported in 2019 [6]. The World Health Organization is working towards zero human transmissions of HAT caused by *T. b. gambiense* (gHAT) by 2030 [7]. Current public health initiatives to control the disease depend on case detection and treatment, complemented with vector control.

Prospects for developing a vaccine are severely confounded by the ability of African trypanosomes to alter their surface antigens [8]. As *T. brucei* persists extracellularly in blood, lymph, and tissue fluids, it is constantly exposed to host antibodies [9–12]. The parasite periodically changes its dense Variant Surface Glycoprotein (VSG) coat to evade immune recognition. This process, called antigenic variation, relies on a vast collection of thousands of VSG-encoding genes[13–16]. *T. brucei* also continually expands the number of usable antigens by constructing mosaic *VSGs* through one or more recombination events between individual *VSG* genes [17,18].

The VSG contains two domains: a variable N-terminal domain of ~350-400 amino acids, and a less variable C-terminal domain of ~40-80 amino acids, characterized by one or two conserved groups of four disulfide-bonded cysteines [13,19]. On the surface of trypanosomes, the VSG N-terminal domain is readily exposed to the host. In contrast, the C-terminal domain is proximal to the plasma membrane and largely hidden from host antibodies [20–22]. The N-terminal domain is classified into two types, A and B, each further distinguished into subtypes (A1-3 and B1-2), while the C-terminal domain has been classified into six types (1-6) [13,19]. These classifications are based on protein sequence patterns anchored by the conservation of cysteine residues, but the biological implications of VSG domain types have not been investigated.

Little is known about how the large genomic repertoire of *VSGs* is used in natural infections; the number and diversity of *VSGs* expressed by wild parasite populations remain unknown. One VSG in particular, LiTat 1.3, has been identified as an antigen against which many gHAT patients have antibodies [23]. As a result, LiTat 1.3 is the main target antigen in the primary serological screening tool for gHAT: the card agglutination test for trypanosomiasis (CATT/*T.b. gambiense*) [24]. Despite the widespread use of the CATT to screen for gHAT, there are shortcomings. Most notably, it relies on immunity against a variable antigen, and some *T. b. gambiense* strains lack the LiTat 1.3 gene entirely [25,26]. More recently developed rapid diagnostic tests use a

combination of native LiTat1.3 and another VSG, LiTat1.5 [27,28], or the combination of a VSG with the invariant surface glycoprotein ISG 65 [29]. Currently, there is no serological test for diagnosis of infection with *T. b. rhodesiense.*

Given the role of VSGs during infection and their importance in gHAT screening tests, a better understanding of *VSG* expression dynamics could inform the development of improved screening tests while providing insight into the molecular mechanisms of antigenic variation. We developed VSG-seq, a targeted RNA-sequencing method that identifies the *VSGs* expressed in any population of *T. brucei* and measures the prevalence of each VSG in the population [30]. In a proof-of-principle study, we used VSG-seq to gain insight into the number and diversity of *VSGs* expressed during experimental mouse infections [30]. This proof-of-principle study revealed significant *VSG* diversity within parasite populations in each animal, with many more variants expressed at a time than the few thought to be sufficient for immune evasion. This diversity suggested that the parasite's genomic VSG repertoire might be insufficient to sustain a chronic infection, highlighting the potential importance of the recombination mechanisms that form new VSGs[13,17]. The study also showed that many of the same *VSGs* were expressed in different infections, supporting previous reports of a "semi-predictable" order to *VSG* switching in *T. brucei* culture and animal models of infection [17,31,32].

Recently, similar high-throughput sequencing methods have been used to characterize antigenic variation in experimental infections of natural hosts for two related African trypanosome species, *T. vivax* and *T. congolense* [33–35]. These studies suggest that the mechanism for antigen production in some animal parasites may be different from the *T. brucei* model. It remains unknown whether findings from studies of antigenic variation using experimental models translate to natural *T. brucei* infections. To our knowledge, only one study has investigated *VSG* expression in wild *T. brucei* isolates [36]. For technical reasons, this study relied on RNA isolated from parasites passaged through small animals after collection from the natural host. As *VSG* expression may change during passage, the data obtained from these samples is somewhat difficult to interpret. To better understand the characteristics of antigenic variation in natural *T. brucei* infections, we sought to analyze *VSG* expression in *T. brucei* field isolates from which RNA was directly extracted.

In the present study, we used VSG-seq to determine the number and diversity of *VSGs* expressed by *T. b. gambiense* in the blood of 12 patients with a *T. b. gambiense* infection. To complement these data, we also analyzed published datasets from both experimental mouse infections and *T. b. rhodesiense* patients. Our analysis revealed diverse expression of *VSGs* in natural *T. brucei* infections and distinct biases in *VSG* expression that may be unique to the *T. b. gambiense* subspecies.

Methods

Ethics statement

The blood specimens from *T.b. gambiense* infected patients were collected within the projects, “Longitudinal follow-up of CATT seropositive, trypanosome negative individuals (SeroSui)” and “An integrated approach for identification of genetic determinants for susceptibility for trypanosomiasis (TrypanoGEN)” [37]. In France, the SeroSui study received approval from the Comité Consultatif de Déontologie et d’Ethique (CCDE) of the French National Institute for Sustainable Development Research (IRD), May 2013 session. In Belgium, the study received approval from the Institutional Review Board of the Institute of Tropical Medicine (reference 886/13) and the Ethics Committee of the University of Antwerp (B300201318039). In the Democratic Republic of the Congo, the projects SeroSui and TrypanoGEN were approved by the Ministry of Health through the Ngaliema Clinic of Kinshasa (references 422/2013 and 424/2013). Participants gave their written informed consent to participate in the projects. For minors, additional written consent was obtained from their legal representative.

Patient enrollment and origin map

Patients originated from the Democratic Republic of the Congo (DR Congo) and were identified over six months in the second half of 2013. This identification occurred either during passive screening at the center for HAT diagnosis and treatment at the hospital of Masi Manimba, or during active screening by the mobile team of the national sleeping sickness control program (PNLTHA) in Masi Manimba and Mosango health zones (Kwilu province, DR Congo).

Individuals were screened for the presence of specific antibodies in whole blood with the CATT test. For those reacting blood positive in CATT, we also tested twofold serial plasma dilutions of 1/2-1/32 were also tested and determined the CATTCATT end titer was determined. CATTCATT positives underwent parasitological confirmation by direct microscopic examination of lymph (if enlarged lymph nodes were present), and examination of blood by the mini-anion exchange centrifugation technique on buffy coat [38]. Individuals in whom trypanosomes were observed underwent lumbar puncture. The cerebrospinal fluid was examined for white blood cell count and the presence of trypanosomes to determine the disease stage and select the appropriate treatment. Patients were questioned about their place of residence. The geographic coordinates of their corresponding villages were obtained from the Atlas of HAT [39] and plotted on a map of the DR Congo using ArcGIS® software by Esri. Distances were determined and a distance matrix generated (see Supplemental Table 2).

Patient blood sample collection and total RNA isolation

A 2.5 mL volume of blood was collected from each patient in a PAXgene Blood RNA Tube. The blood was mixed with the buffer in the tube, aliquoted in 2 mL volumes and frozen in liquid nitrogen for a maximum of two weeks. After arrival in Kinshasha, tubes

were stored at -70°C. Total RNA was extracted and isolated from each blood sample as previously described [40].

Estimation of parasitemia

Two approaches were used to estimate parasitemia. First, a 9 mL volume of blood on heparin was centrifuged, 500 microliters of the buffy coat were taken up and trypanosomes were isolated using the mini-anion exchange centrifugation technique. After centrifugation of the column eluate, the number of parasites visible in the tip of the collection tube were estimated. Second, Spliced Leader (SL) RNA expression levels were measured by real-time PCR as previously described [40]. A Ct value was determined for each patient blood sample. Real-time PCR was performed on RNA samples before reverse transcription to verify the absence of DNA contamination.

RNA sequencing

DNase I-treated RNA samples were cleaned up with 1.8x Mag-Bind TotalPure NGS Beads (Omega Bio-Tek, # M1378-01). cDNA was generated using the SuperScript III First-strand synthesis system (Invitrogen, 18080051) according to manufacturer's instructions. 8 microliters of each sample (between 36 and 944 ng) were used for cDNA synthesis, which was performed using the oligo-dT primer provided with the kit. This material was cleaned up with 1.8x Mag-Bind beads and used to generate three replicate library preparations for each sample. These technical replicates were generated to ensure that any *VSGs* detected were not the result of PCR artifacts[41,42].

Because we expected a low number of parasites in each sample, we used a nested PCR approach to prepare the VSG-seq libraries. First, we amplified *T. brucei* cDNA from the parasite/host cDNA pool by PCR using a spliced leader primer paired with an anchored oligo-dT primer (SL-1-nested and anchored oligo-dT; Supplemental Table 1). 20 cycles of PCR were completed (55ºC annealing, 45s extension) using Phusion polymerase (Thermo Scientific, #F530L). PCR reactions were cleaned up with 1.8x Mag-Bind beads. After amplifying *T. brucei* cDNA, a *VSG*-specific PCR reaction was carried out using M13RSL and 14-mer-SP6 primers (see primers; Supplemental Table 1). 30 cycles of PCR (42ºC annealing, 45s extension) were performed using Phusion polymerase. Amplified *VSG* cDNA was then cleaned up with 1X Mag-Bind beads and quantified using a Qubit dsDNA HS Assay (Invitrogen Q32854).

Sequencing libraries were prepared from 1 ng of each VSG PCR product using the Nextera XT DNA Library Preparation Kit (Illumina, FC-131-1096) following the manufacturer's protocol except for the final cleanup step, which was performed using 1X Mag-Bind beads. Single-end 100bp sequencing was performed on an Illumina HiSeq 2500. Raw data are available in the National Center for Biotechnology Information (NCBI) Sequence Read Archive under accession number PRJNA751607.

VSG-seq analysis of *T. b. gambiense* and *T. b. rhodesiense* sequencing libraries

To analyze both *T. b. gambiense* (VSG-seq preparations) and *T. b. rhodesiense* (traditional mRNA sequencing library preparations; sequences were obtained from ENA, accession numbers PRJEB27207 and PRJEB18523), we processed raw reads using the VSG-seq pipeline available at https://github.com/mugnierlab/VSGSeqPipeline. Briefly, *VSG* transcripts were assembled *de novo* from quality- and adapter-trimmed reads for each sample (patient or patient replicate) from raw reads using Trinity (version 5.26.2) [43]. Contigs containing open reading frames (ORFs) were identified as previously described [30]. ORF-containing contigs were compared to Lister 427 and EATRO1125 *VSGs* as well as a collection of known contaminating non-*VSG* sequences. Alignments to *VSGs* with an E-value below $1x10^{-10}$ that did not match any known non-*VSG* contaminants were identified as *VSG* transcripts. For *T. b. gambiense* replicate libraries, *VSG* ORFs identified in any patient replicate were consolidated into a sole reference genome for each patient using CD-HIT (version 4.8.1)[44] with the following arguments: -d 0 -c 0.98 -n 8 -G 1 -g 1 -s 0.0 -aL 0.0. Final *VSG* ORF files were manually inspected.

Two *T. b. gambiense* patient *VSG*s (Patients 11 and 13) showed likely assembly errors. In one case, a *VSG* was duplicated and concatenated, and in another, two *VSGs* were concatenated. These reference files were manually corrected (removing the duplicate or editing annotation to reflect two *VSGs* in the concatenated ORF) so that each *VSG* could be properly quantified. *VSG* reference databases for each patient are available at https://github.com/mugnierlab/Tbgambiense2021/. For *T. b. gambiense,* we then aligned reads from each patient replicate to that patient's consolidated reference genome using Bowtie with the parameters *-v 2 -m 1 -S* (version 1.2.3) [45].

For *T. b. rhodesiense,* we aligned each patient's data to its own *VSG* ORF assembly. RPKM values for each *VSG* in each sample were generated using MULTo (version 1.0) [46], and the percentage of parasites in each population expressing a *VSG* was calculated as described previously [30]. For *T. b. gambiense* samples, we included only *VSGs* with an expression measurement above 1% in two or more patient replicates in our analysis. For *T. b. rhodesiense* samples, we included only *VSGs* with expression >0.01%. To compare *VSG* expression between patients, despite the different reference genomes used for each patient, we used CD-HIT to cluster *VSG* sequences with greater than 98% similarity among patients, using the same parameters used to consolidate reference *VSG* databases before alignment. We gave each unique *VSG* cluster a numerical ID (e.g., Gambiense #) and chose the longest sequence within each group to represent the cluster. Before analysis, we manually removed clusters representing TgsGP and SRA from the expressed *VSG* sets. UpSet plots were made with the UpSetR package[47]. The R code used to analyze resulting data and generate figures is available at https://github.com/mugnierlab/Tbgambiense2021/.

293 **Analysis of VSG N-terminal domains**
294
295 Genomic *VSG* sequences
296 The *VSG* repertoires of *T. b. brucei* Lister 427 ("Lister427_2018" assembly), *T. b. brucei*
297 TREU927/4 and *T. b. gambiense* DAL972 were taken from TriTrypDB (v50), while the
298 *T. b. brucei* EATRO 1125 VSGnome was used for analysis of the EATRO1125 *VSG*
299 repertoire (vsgs_tb1125_nodups_atleast250aas_pro.txt, available at
300 https://tryps.rockefeller.edu/Sequences.html or GenBank accession KX698609.1 -
301 KX701858.1). VSG sequences from other strains (except those generated by VSG-seq)
302 were taken from the analysis in Cross, et al. [15]. Likely VSG N-termini were identified
303 as predicted proteins with significant similarity (e-value ≤ 10^{-5}) to hidden Markov models
304 (HMMs) of aligned type A and B VSG N-termini taken from [15].
305
306 N-terminal domain phylogenies
307 Phylogenies of VSG N-termini based on unaligned sequence similarities were
308 constructed using the method described in [48] and used previously to classify VSG
309 sequence [15]. We extracted predicted N-terminal domain protein sequences by using
310 the largest bounding envelope coordinates of a match to either type A or type B HMM. A
311 matrix of similarities between all sequences was constructed from normalized
312 transformed BLASTp scores as in Wickstead, et al. [48] and used to infer a neighbor-
313 joining tree using QuickTree v1.1 [49]. Trees were annotated and visualized in R with
314 the package APE v5.2 [50].
315
316 HMM
317 For N-terminal typing by HMM, we used a python analysis pipeline available at
318 (https://github.com/mugnierlab/find_VSG_Ndomains). The pipeline first identifies the
319 boundaries of the VSG N-terminal domain using the type A and type B HMM profiles
320 generated by Cross *et al.* which includes 735 previously-typed VSG N-terminal domain
321 sequences [15]. N-terminal domains are defined by the largest envelope domain
322 coordinate that meets e-value threshold ($1x10^{-5}$, --domE 0.00001). In cases where no
323 N-terminal domain is identified using these profiles, the pipeline executes a "rescue"
324 domain search in which the VSG is searched against a 'pan-VSG' N-terminus profile we
325 generated using 763 previously-typed VSG N-terminal domain sequences. This set of
326 VSGs includes several *T. brucei* strains and/or subspecies: Tb427 (559), TREU927
327 (138), *T. b. gambiense* DAL972 (28), EATRO795 (8), EATRO110 (5), *T. equiperdum*
328 (4), and *T. evansi* (21). The N-terminal domain type of these VSGs were previously
329 determined by Cross et. al (2014) by building neighbor-joining trees using local
330 alignment scores from all-versus-all BLASTp similarity searches [15]. Domain
331 boundaries are called using the same parameters as with the type A and B profiles.
332
333 After identifying boundaries, the pipeline extracts the sequence of the N-terminal
334 domain, and this is searched against five subtype HMM profiles. To generate N-terminal
335 domain subtype HMM profiles, five multiple sequence alignments were performed using
336 Clustal Omega [51] with the 763 previously-typed VSG N-terminal domain sequences
337 described above; each alignment included the VSG N-terminal domains of the same
338 subtype (A1, A2, A3, B1, and B2). Alignment output files in STOCKHOLM format were

339 used to generate distinct HMM profiles for type A1, A2, A3, B1, and B2 VSGs using the
340 pre-determined subtype classifications of the 763 VSGs using HMMer version 3.1b2
341 [52]. The number of sequences used to create each subtype profile ranged from 75 to
342 211. The most probable subtype is determined by the pipeline based on the highest
343 scoring sequence alignment against the subtype HMM profile database when HMMscan
344 is run under default alignment parameters. The pipeline generates a FASTA file
345 containing the amino acid sequence of each VSG N-terminus and a CSV with
346 descriptions of the N-terminal domain including its type and subtype.
347
348 Network graph
349 N-terminal network graphs were made using VSG N-terminal domains from the
350 TriTrypDB Lister427_2018 and *T. b. gambiense* DAL972 (v50) VSG sets described
351 above, and the *T. b. gambiense* and *T. b. rhodesiense* patient VSG N-termini which met
352 our expression thresholds. Identified N-terminal domains were then subjected to an all-
353 versus-all BLASTp. A pairwise table was created that includes each query-subject pair,
354 the corresponding alignment E-value, and N-terminal domain type of the query
355 sequence if previously typed in Cross, et al. [15]. Pseudogenes and fragments were
356 excluded from the Lister427_2018 reference prior to plotting by filtering for *VSG* genes
357 annotated as pseudogenes and any less than 400 amino acids in length, as the
358 remaining sequences are most likely to be full length VSG. Network graphs were
359 generated with the igraph R package[53] using undirected and unweighted clustering of
360 nodes after applying link cutoffs based on E-value < 10^{-2}. The leading eigenvector
361 clustering method [54] was used to detect and assign nodes to communities based on
362 clustering (cluster_leading_eigen() method in igraph).
363
364
365 **Analysis of VSG C-terminal domains**
366 VSG C-termini were extracted from expressed *T. b. gambiense VSGs*, *T.b. gambiense*
367 DAL972 (v50), and 545 previously-typed VSG C-termini from the Lister 427 strain using
368 the C-terminal HMM profile generated by Cross et al.[15] and the same HMMscan
369 parameters as for N-termini (E-value < $1x10^{-5}$; largest domain based on envelope
370 coordinates). An all-vs-all BLASTp was performed on these sequences, and network
371 graphs were generated in the same manner as the N-terminal network graphs. Links
372 were drawn between C-termini with a BLASTp E-value $1x10^{-3}$. The leading eigenvector
373 method for clustering [54] was used to detect and assign nodes to communities based
374 on clustering (cluster_leading_eigen() method in igraph).
375
376
377 **Comparison of gHAT patient VSGs to the DAL972 reference**
378 The nucleotide sequences of expressed *T. b. gambiense* patient VSGs were compared
379 to the complete *T. b. gambiense* DAL972 reference genome sequence (v54) from
380 TriTrypDB using BLASTn. To find evidence of VSG diversification by mosaicism or
381 segmental gene conversion, permissive parameters were used so short regions of
382 homology would be reported (blastn -word_size 11 -evalue 0.1). Both query and subject
383 alignment coordinates were recorded in the output for downstream analysis, along with

384 E-value and percent identity. Alignment ranges were plotted with the IRanges R
385 package[55].

386 # Results
387
388 **Parasites in gHAT patients express diverse sets of VSGs**
389
390 To investigate *VSG* expression in natural human infections, we performed VSG-seq on
391 RNA extracted from whole blood collected from 12 human African trypanosomiasis
392 patients from five locations in the Kwilu province of DR Congo (Figure 1A). We
393 estimated the relative parasitemia of each patient by SL-QPCR [56], and we estimated
394 the number of parasites after mAECT on buffy coat for all patients except patient 29
395 (Table 1). Using RNA extracted from 2.5 mL of whole blood from each patient, we
396 prepared libraries for VSG-seq in three separate batches for each technical replicate.
397 We amplified *T. brucei* RNA from host/parasite total RNA using a primer against the *T.*
398 *brucei* spliced leader sequence and an anchored oligo-dT primer. The resulting
399 trypanosome-enriched cDNA was used as a template to amplify *VSG* cDNA, and *VSG*
400 amplicons were then submitted to VSG-seq sequencing and analysis. To determine
401 whether a *VSG* was expressed within a patient, we applied the following stringent
402 cutoffs:
403
404 1) We conservatively estimate that each 2.5 mL patient blood sample contained
405 a minimum of 100 parasites. At this minimum parasitemia, a single parasite
406 would represent 1% of the population (and consequently ~1% of the parasite
407 RNA in a sample). As a result, we excluded all *VSGs* expressed by <1% of
408 the population as estimated by VSG-seq.
409 2) We classified *VSGs* as expressed if they met the expression cutoff in at least
410 two of three technical library replicates.
411
412 1112 unique *VSG* open reading frames were assembled *de novo* in the patient set and
413 44 met our expression criteria. Only these 44 *VSGs*, which we will refer to as
414 "expressed *VSGs,"* were considered in downstream analysis, except when otherwise
415 noted. TgsGP, the VSG-like protein which partially enables resistance to human serum
416 in *T. b. gambiense* [57], assembled in samples from patients 2, 11, 13, and 17, and met
417 the expression threshold in patients 2, 11, and 17. The absence of this transcript in
418 most samples is likely due to the low amount of input material used to prepare samples.
419 Notably, none of the expressed *VSGs* shared significant nucleotide sequence similarity
420 outside the conserved C-terminal domain with any *VSGs* in the *T. b. gambiense*
421 DAL972 genome (Supplemental Figures 6 and 7).
422
423 At least one *VSG* met our expression criteria in each patient, and in most cases,
424 multiple *VSGs* were detected. Patient 2 showed the highest diversity, with 14 *VSGs*
425 expressed (Figure 1B, Supplemental Figure 1). We observed a correlation between
426 parasitemia, as estimated by qPCR, and the number of *VSGs* (Supplemental Figure 2),
427 suggesting that these samples do not reflect the full diversity of each population.
428 Nevertheless, two *VSGs* were shared between patients: *VSG* 'Gambiense 195' was
429 expressed in both patient 12 and patient 17 from Village C; *VSG* 'Gambiense 38' was
430 expressed in patient 12 from Village C and patient 23 from Village D (Figure 1C).
431 Because our sampling did not reach saturation, resulting in some variability between

technical replicates, we chose to focus only on the presence/absence of individual VSGs rather than relative expression levels within each population.

Patient	Location	est. parasites in 500µL buffy coat	mean SL-RNA Ct	WBC	Parasites in CSF	Stage
1	Village A	>50	22.155	1	-	First
2	Village A	>50	19.020	6	-	Early 2nd
3	Village A	2-5	28.780	6	-	Early 2nd
11	Village C	>50	22.030	9	-	Early 2nd
12	Village C	6-20	25.430	6	-	Early 2nd
13	Village C	6-20	26.635	12	-	Early 2nd
17	Village C	21-50	24.495	13	-	Early 2nd
19	Village C	1	28.245	7	-	Early 2nd
23	Village D	6-20	27.085	2	-	First
29	Village B	-	28.320	3	-	First
30	Village B	>50	22.960	694	+	Severe 2nd
33	Village E	1	32.385	2	-	First

Table 1. Patient stage and parasitemia data. We used the following staging definitions: First: 0-5 WBC/µl, no trypanosomes in cerebrospinal fluid (CSF). Second: >5 WBC/µl or trypanosomes in CSF (with early 2nd: 6-20 WBC/µl and no trypanosomes in CSF; severe 2nd: >100 WBC/µl). WBC: white blood cells.

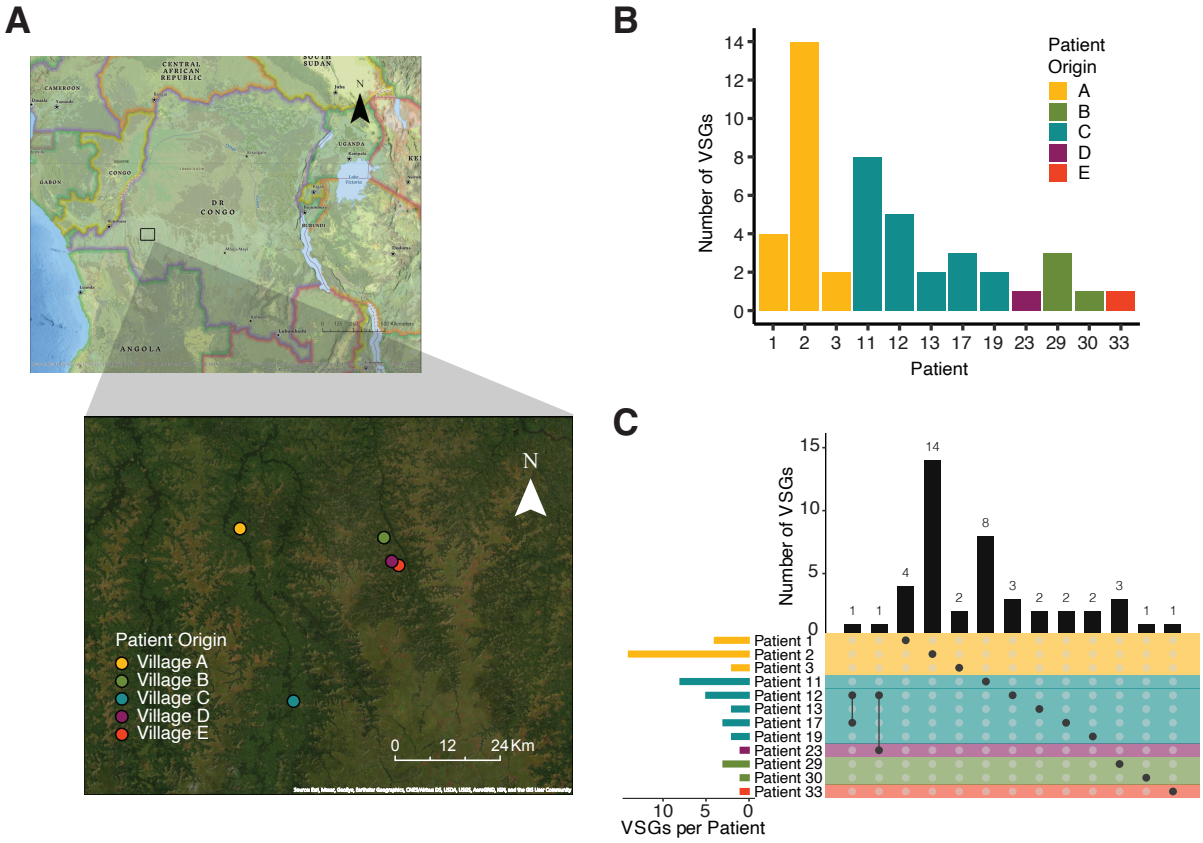

Figure 1. Parasites isolated from gHAT patients express multiple *VSGs*. (A) Map showing the location of each patient's home village. Maps were generated with ArcGIS® software by Esri, using world imagery and National Geographic style basemaps. (B) Graph depicting the total number of *VSGs* expressed in each patient. (C) The intersection of expressed *VSG* sets in each patient. Bars on the left represent the size of the total set of VSGs expressed in each patient. Dots represent an intersection of sets with bars above the dots representing the size of the intersection. Color indicates patient origin.

453 **Natural *T. b. gambiense* infections show a strong bias towards the expression of**
454 **type B VSG**
455
456 To further characterize the set of expressed *VSGs* in these samples, we sought a fast
457 and unbiased method for determining the type and subtype of each VSG's N-terminal
458 domain. We evaluated two approaches. The first approach was to create a bioinformatic
459 pipeline to determine each N-terminal domain subtype, using HMM profiles we created
460 for each subtype from sets of N-terminal domains previously typed by Cross et al. [15].
461 The second approach was to create a BLASTp network graph based on a published
462 method [58] where the N-terminal subtype of a VSG is determined by the set of VSGs it
463 clusters with, and clusters are identified using the leading eigenvector method [54]. We
464 used each approach to determine the N-terminal subtype of each expressed *VSG* in our
465 patient sample dataset, along with 863 VSG N-termini from the Lister 427 genome. We
466 compared these results to either existing N-terminal classification (for Lister 427 VSGs)
467 or classification based on position in a newly-generated BLASTp-tree [15] (for *T. b.*
468 *gambiense* VSGs; Figure 2A).
469
470 Both the new HMM profile and BLASTp network graph approaches generally
471 recapitulated previous VSG classification based on BLASTp-tree, with all three methods
472 agreeing 93.7% of the time (Figure 2B). The HMM pipeline method agreed with
473 BLASTp-tree typing for all patient VSGs, while the network graph approach agreed for
474 43/44 VSGs (Figure 2B, Supplemental Figure 3, Supplemental Table 1) [15]. It is not
475 surprising that the HMM pipeline would better reflect the results of the BLASTp-tree
476 method, as the N-terminal subtype HMM profiles were generated using VSGs classified
477 by this method. Based on these data, we determined that the HMM method is a fast and
478 accurate approach for determining the N-terminal domain types of unknown VSGs.
479
480 Our N-terminal domain typing pipeline identified the domain sequence and subtype for
481 all 44 patient VSGs (Figure 2C). Of the expressed *T. b. gambiense* VSGs, 82% had
482 type B N-terminal domains, and 50% or more of expressed *VSGs* within each patient
483 were type B. This bias was not restricted to highly expressed *VSGs*, as 74.5% of all
484 assembled *VSG* (813 of 1091 classifiable to an N-terminal subtype) were also type B.
485 This observation motivated further investigation into the expressed N-terminal domains
486 in infections by other *T. brucei* subspecies.
487

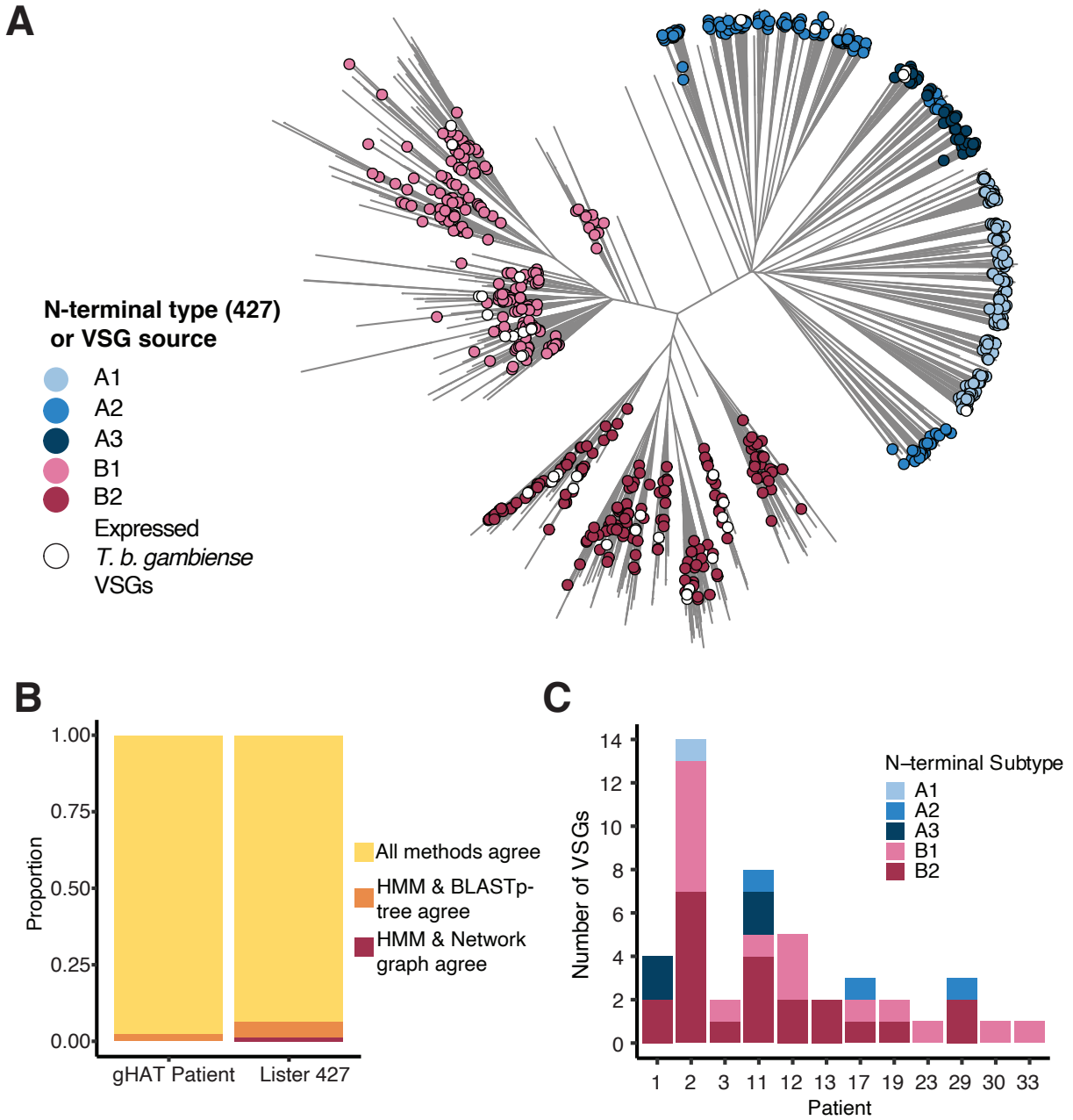

Figure 2. *T. b. gambiense* samples show a bias towards the expression of type B VSG. (A) Visualization of relatedness between N-terminal domain peptide sequences inferred by Neighbor-Joining based on normalized BLASTp scores. Legend indicates classification by HMM pipeline (for Lister 427 VSGs, to highlight agreement between the two methods) or by subspecies for *VSGs* expressed in patients. (B) Agreement between three VSG typing methods for Lister 427 *VSG* set and the expressed *T. b. gambiense* patient *VSG* set. (C) N-terminal domain subtype composition of expressed *T. b. gambiense VSGs* as determined by HMM analysis pipeline.

500 **Type B VSG bias is not observed in natural *T. b. rhodesiense* infection**
501
502 To determine whether the bias towards type B VSGs was unique to *T. b. gambiense*
503 infections, we analyzed RNA-seq data from a published study measuring gene
504 expression in the blood and cerebrospinal fluid (CSF) of *T. b. rhodesiense* patients in
505 Northern Uganda [59]. These libraries were prepared conventionally after either rRNA-
506 depletion for blood or poly-A selection for CSF samples. We analyzed only those
507 samples for which at least 10% of reads mapped to the *T. brucei* genome. Raw reads
508 from these samples were subjected to the VSG-seq analysis pipeline. Because the
509 estimated parasitemia of these patients was much higher than our *T. b. gambiense*
510 study, we adjusted our expression criteria accordingly to 0.01%, the published limit of
511 detection of VSG-seq [30]. Using this approach, we identified 77 unique *VSG*
512 sequences across all blood and CSF samples (Figure 3A, Supplemental Figure 4).
513 SRA, the VSG-like protein that confers human serum resistance in *T. b. rhodesiense*
514 [60], was expressed in all patient samples.
515
516 The HMM pipeline determined types for 74 of these VSG sequences; the remaining
517 sequences appeared to be incompletely assembled, presumably due to insufficient read
518 depth from their low level of expression. Multiple *VSGs* assembled in each patient
519 (Figure 3A), and a large proportion of *VSGs* were expressed in multiple patients (Figure
520 3C), in line with our observations in experimental mouse infections. Although most
521 VSGs detected in these patients were type B (57%, Figure 3B), this VSG type was
522 much less predominant than in *T. b. gambiense* infection. Interestingly, *T. b.*
523 *rhodesiense* patient CSF revealed another possible layer of diversity in *VSG*
524 expression, with 5 *VSGs* expressed exclusively in this space.
525
526
527
528

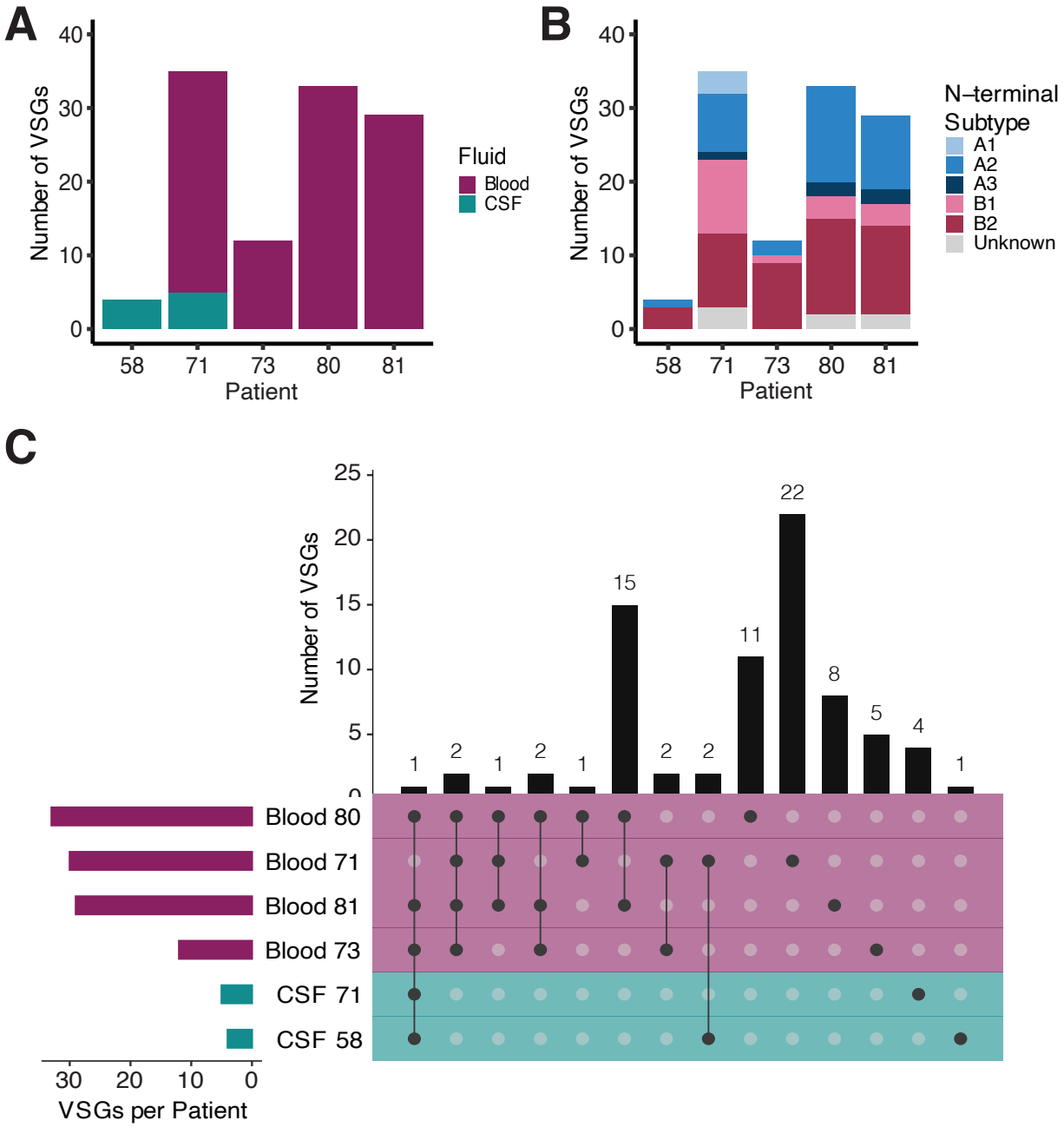

Figure 3. *T. b. rhodesiense* samples reveal diverse *VSG* expression but little N-terminal type bias. (A) The total number of expressed *T. b. rhodesiense VSGs* in each patient and sample type. Bar color represents the sample type from which RNA was extracted. (B) N-terminal domain subtype composition of all expressed *VSGs*. (C) Intersections of *VSGs* expressed in multiple infections. Bars on the left represent the size of the total set of VSGs expressed in each patient. Dots represent an intersection of sets, with bars above the dots representing the size of the intersection. Color indicates patient origin.

539 **The predominant VSG N-terminal type fluctuates over time during experimental *T.***
540 ***b. brucei* infection**
541
542 One explanation for the bias towards type B VSG in *T. b. gambiense* could be that VSG
543 type stabilizes over time and type B predominates at later infection timepoints. This
544 explanation is plausible because patient samples only represent a single moment during
545 infection, and *T. b. gambiense* samples are more likely to be obtained at much later
546 timepoints post-infection. To investigate whether N-terminal type predominance is
547 stable or fluctuates over the course of infection, we took advantage of our published
548 VSG-seq analysis of parasites isolated from mice infected with the *T.b. brucei*
549 EATRO1125 strain. Blood was collected over time during this study, providing data from
550 days 6/7, 12, 14, 21, 24, 26, and 30 post-infection in all four mice, and from days 96, 99,
551 102, and 105 in one of the four mice (Mouse 3). Of 192 unique VSGs identified between
552 days 0-30, the python HMM pipeline typed 190; of 97 unique VSGs identified between
553 days 96-105, the pipeline typed 93 VSGs. The remaining VSGs were incompletely
554 assembled by Trinity. Our analysis of VSG types over time revealed that the
555 predominantly expressed N-terminal domain type fluctuates between type A and type B
556 throughout the early stages of infection and in extended chronic infections (Figure 4).
557 Parasitemia did not correlate with either the diversity of *VSG* expression or N-terminal
558 domain type predominance (Supplemental Figure 3). Because all patient samples were
559 collected from a single timepoint in varying stages of disease, it remains unclear
560 whether the predominant N-terminal type continues to fluctuate in human infections over
561 time as it does in mice that have reached chronic stages of infection.
562

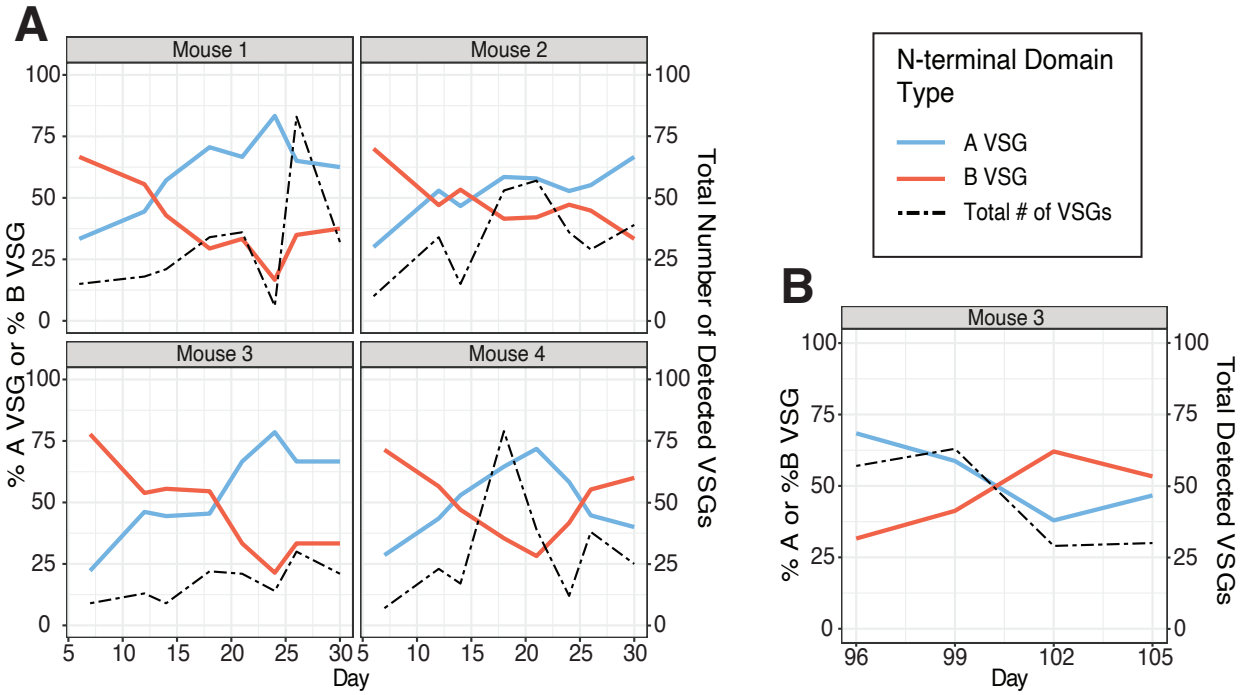

Figure 4. VSG N-terminal type composition fluctuates over the course of infection in mice. Proportions of N-terminal domain types expressed in *T. b. brucei* infected mice over time. The black dotted line represents the total number of identified VSGs. A) N-terminal type composition days 0-30. B) Type composition days 96-105.

The composition of the genomic VSG repertoire is reflected in expressed VSG N-terminal domain types

Another source for bias in expressed VSG type is the composition of the genomic *VSG* repertoire. We could directly compare the genomic and expressed *VSG* repertoire for EATRO1125 mouse infections, as the 'VSGnome' for this strain has been sequenced. Although the predominant N-terminal VSG type fluctuates throughout these infections, the expressed *VSG* repertoire across all time points generally reflects the composition of the genomic repertoire (chi-squared p = 0.0515, Figure 5A).

Unfortunately, the entire repertoire of *VSGs* encoded by most trypanosome strains is unknown, so such a direct comparison is impossible for *T. b. gambiense* and *T. b. rhodesiense* patient samples. Although the content of the 'core' *T. brucei* genome (containing the diploid, housekeeping genes) is similar enough among subspecies for resequencing projects to be scaffolded using the TREU927 or Lister 427 reference genomes [61–63], it is not clear whether the *VSG* repertoires of subspecies (or even individual parasite strains [36]) share this degree of similarity. Because no near-complete VSGnome for any *T. b. rhodesiense* strain was available, we compared the makeup of *T. b. rhodesiense* expressed *VSGs* with the closely related and near-complete *T. b. brucei* Lister 427 repertoire [62]. We observed no difference in the proportions of N-terminal types (chi-squared p-value = 0.2422) (Figure 5B). Similarly, the proportion of N-terminal domains identified in the *T. b. gambiense* patient samples is not statistically different from the incomplete *T. b. gambiense* DAL972 genomic repertoire (chi-squared p-value = 0.0575) (Figure 5B). Both *T. b. gambiense* patient VSGs (chi-squared p-value = 2.413e-4) and the 54 VSGs identified in *T. b. gambiense* DAL972 (chi-square p-value = 0.0301) have A and B type frequencies that differ significantly from Lister427. These results should be interpreted with caution given the limitations of the reference genomes used. Taken together, however, they support a model in which VSG types are drawn from the repertoire at a roughly equal frequency to their representation in the genome, with *T. b. gambiense* exhibiting an N-terminal type composition that differs from other subspecies.

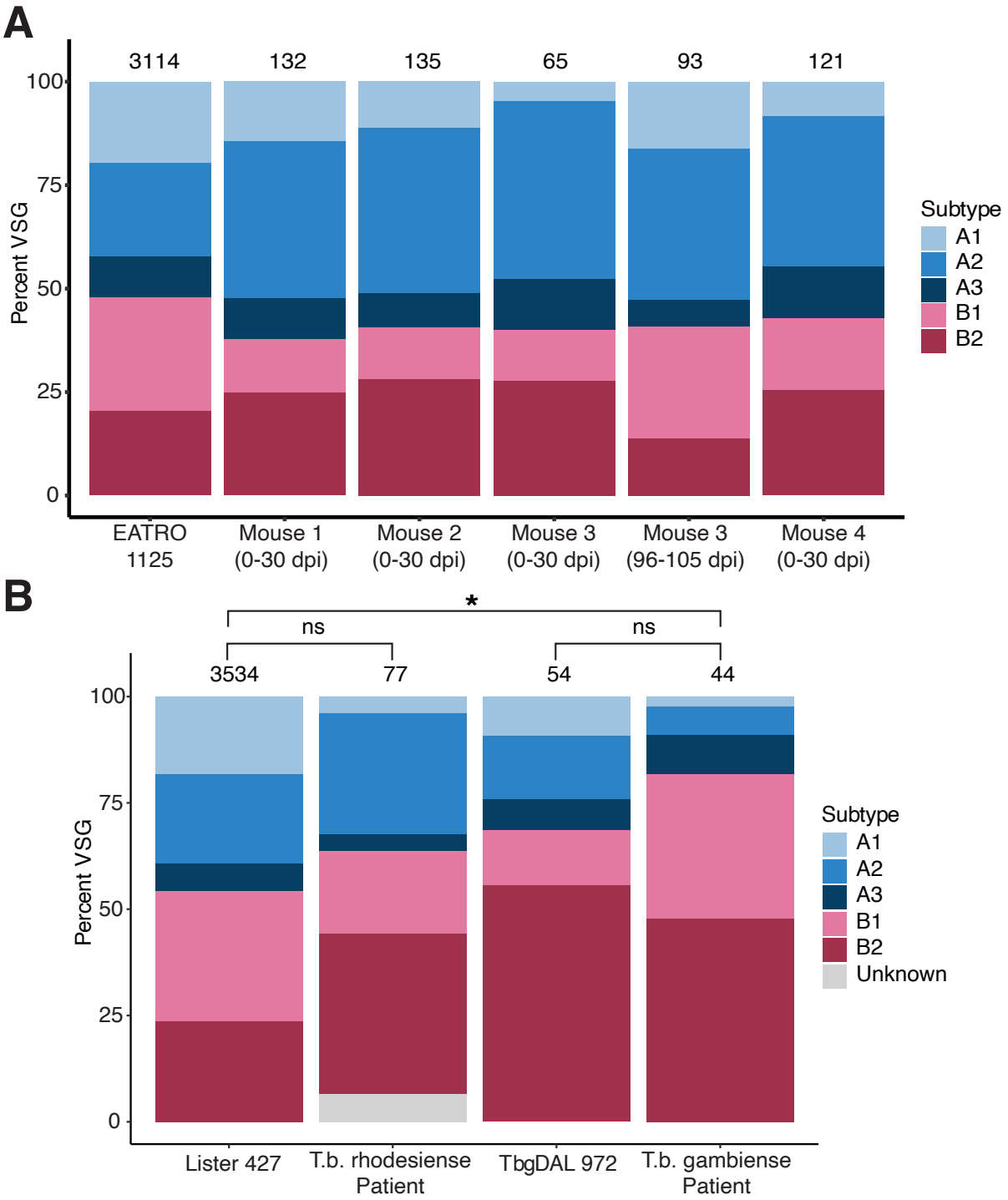

601

602 **Figure 5. VSG expression reflects the genomic VSG repertoire of the infecting parasites.**
603 (A) Columns show the proportion of VSG types identified in each mouse infection over all time
604 points and the proportion of VSG types in the infecting *T. b. brucei* strain, EATRO 1125. The
605 total number of unique VSG sequences is displayed above each column. (B) A comparison of
606 the frequencies of type A and B VSGs expressed in patients and those present in Lister 427 and
607 DAL972 reference genomes. Relevant statistical comparisons are shown.

608
609 ***T. b. gambiense* expressed VSG C-terminal domains show a bias for type 2**
610 **domains**
611
612 In addition to examining N-terminal types in our *T. b. gambiense* dataset, we also
613 examined expressed VSG C-termini. Previous studies defined six C-terminal types,
614 although resolving these types in larger VSG sets has been difficult due to the extensive
615 similarity among VSG C-termini [15,58]. In line with previous observations, a BLASTp-
616 tree analysis of assembled *T. b. gambiense* C-terminal domains revealed frequent
617 sequence similarity between expressed C-terminal types but did not provide sufficient
618 resolution to confidently assign types (Fig 6A). To supplement this analysis, we also
619 performed a network graph analysis. Although this method had previously performed
620 poorly in resolving VSG C-termini [58], using the leading eigenvector clustering method
621 [54] to define community membership within the graph allowed a faithful reconstitution
622 of the C-terminal types previously determined by BLASTp-tree analysis.
623
624 Using the network graph approach, we tentatively assigned C-terminal domain types to
625 the *T. b. gambiense* VSGs (Figure 6B). Most patient C-terminal domain types were type
626 2, while the remaining types were predominantly type 1. Only one type 3 C-terminus
627 was identified in the patient set. Although there are very few VSG C-termini available in
628 the *T. b. gambiense* DAL972 genome, these sequences show a predominance of types
629 3 and 5. In contrast, the genomic repertoire of C-termini in Lister 427 shows a roughly
630 equivalent representation of types 1, 2, and 3. Unlike *T. b. gambiense* N-termini, the
631 expressed *T. b. gambiense* C-termini were more restricted than the sets of C-termini
632 apparently available in the *T. b. gambiense* DAL972 or *T. b. brucei* Lister 427 genomes
633 (Fisher's exact test, p-value $< 1x10^{-5}$).
634
635 In line with previous observations, we saw no evidence of domain exclusion: a C-
636 terminal domain of one type could be paired with any type of N-terminal domain (Figure
637 6E)[20]. As observed in our analysis of expressed N-termini, C-terminal domain types
638 were not correlated to geographical origin (Figure 6F). Overall, these data suggest that,
639 like N-termini, expressed VSG C-termini are also biased towards certain C-terminal
640 types. Unlike N-termini, however, C-terminal types expressed in *T. b. gambiense*
641 infection may not reflect the parasite's genomic repertoire composition.

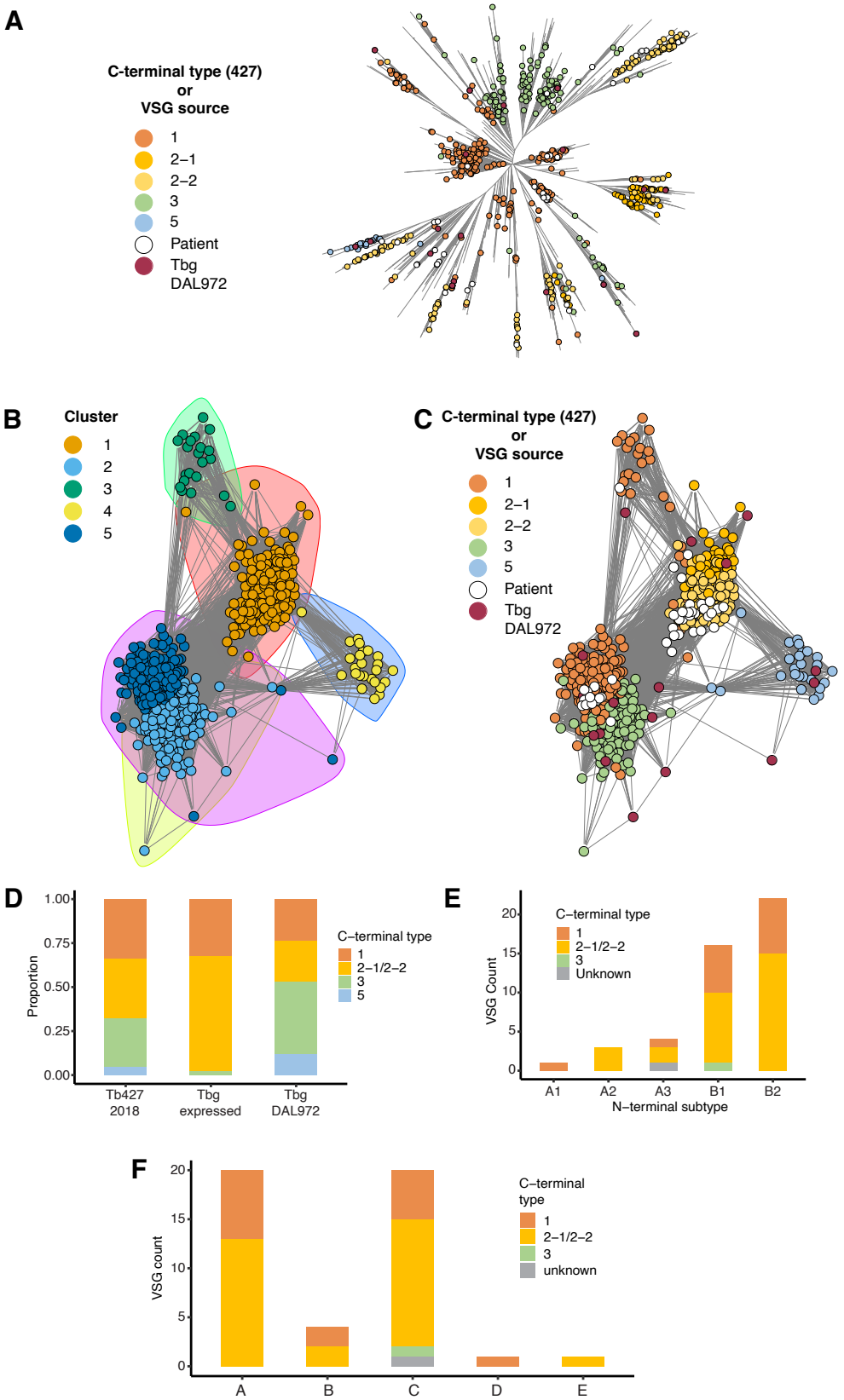
A
C-terminal type (427)
or
VSG source
1
2–1
2–2
3
5
Patient
Tbg
DAL972
B
Cluster
1
2
3
4
5
C
C-terminal type (427)
or
VSG source
1
2–1
2–2
3
5
Patient
Tbg
DAL972
D
Proportion
1.00
0.75
0.50
0.25
0.00
Tb427
2018
Tbg
expressed
Tbg
DAL972
C–terminal type
1
2–1/2–2
3
5
E
VSG Count
20
15
10
5
0
A1
A2
A3
B1
B2
N–terminal subtype
C–terminal type
1
2–1/2–2
3
Unknown
F
VSG count
20
15
10
5
0
A
B
C
D
E
C–terminal
type
1
2–1/2–2
3
unknown

642

643 **Figure 6. Expressed VSG C-termini are primarily type 1 and type 2.** A) BLASTp-tree of C-
644 terminal domains. Points are colored based on previously determined C-terminal type from
645 Cross et al. or by the source of the sequence (genomic or expressed) for *T. b. gambiense*
646 *VSGs*. B) Network plot showing peptide sequence relatedness between C-terminal domains in
647 *T. b. gambiense* expressed VSGs. Each point represents a VSG C-terminus. A link was drawn
648 between points if the BLASTp e-value was less than $1x10^{-3}$. Points are colored by the cluster
649 determined by the clustering algorithm. Shaded circles also indicate clusters. C) Same network
650 plot as in B but colored by previously determined C-terminal type from Cross et al., or by source
651 for unclassified genomic or expressed *VSGs*. D) VSG C-terminal types, based on cluster
652 assignment visualized in panel B, in genomic and expressed *VSG* sets. E) Pairing of C- and N-
653 termini in *T. b. gambiense* patients. F) C-termini detected in each patient village.

Discussion

African trypanosomes evade the host adaptive immune response through a process of antigenic variation where parasites switch their expressed *VSG* [64]. The genome of *T. brucei* encodes a large repertoire of *VSG* genes, pseudogenes, and gene fragments that can be expanded continuously through recombination to form entirely novel "mosaic" *VSGs* [17]. While antigenic variation has been studied extensively in culture and animal infection models, our understanding of the process in natural infections, particularly human infection, is limited. Most experimental mouse infections are sustained for weeks to months, while humans and large mammals may be infected for several months or even years. Additionally, laboratory studies of antigenic variation almost exclusively use *T. b. brucei*, a subspecies of *T. brucei* that, by definition, does not infect humans.

The primary hurdle to exploring antigenic variation in nature has been technical: it is difficult to obtain sufficient parasite material for analysis. This is especially true for infection with *T. b. gambiense,* which often exhibits extremely low parasitemia. VSG-seq, which relies on PCR and requires very small amounts of material for analysis, provides a new tool for exploring *VSG* expression in natural human infections. Here we have demonstrated the feasibility of VSG-seq to analyze *VSG* expression in RNA samples isolated directly from HAT patients. Our analyses show that the diversity seen in mouse infection models is mostly recapitulated in natural infection; however, there may be unique aspects of antigenic variation in *T. b. gambiense* that can only be explored by studying natural infections.

The most notable result in our previous analysis of mouse infections was the diversity of *VSGs* expressed within each infection. Rather than a few *VSGs* expressed at a time, we saw many *VSGs* expressed simultaneously in each parasite population. This finding confirms previous estimates of antigenic diversity in experimental mouse infection [17] and suggests that the genomic *VSG* repertoire might be exploited very rapidly. The study presented here detected several expressed *VSGs* in most *T. b. gambiense* samples. Although diversity in *T. b. gambiense* infection appeared lower overall, the correlation we observed between parasitemia and diversity in *T. b. gambiense* isolates suggests that our sampling was incomplete. Indeed, in our analysis of *T. b. rhodesiense* infection (a more reasonable comparison to mouse infection given similar expression cutoffs and parasitemia), we observed diversity similar to or higher than what we have detected in *T. b. brucei* mouse infections. Moreover, *T. b. rhodesiense* patient CSF revealed another layer of diversity in *VSG* expression, with 5 *VSGs* expressed exclusively in this space. Although this observation is difficult to interpret without information about the precise timing of sample collection, it is exciting to speculate that different organs or body compartments could harbor different sets of VSGs. Overall, our analysis of *VSG* expression in *T. b. gambiense* and *T. b. rhodesiense* patients confirmed the long-held assumption that *VSG* diversity is a feature of natural infection.

While analyzing the sets of expressed *VSGs* in *T. b. gambiense* and *T. b. rhodesiense* infections, we found evidence for another feature of experimental infection that holds

700 true in a natural host: hierarchical *VSG* expression. Both *in vitro* and *in vivo* studies
701 have shown that *VSG* switching is not entirely stochastic but rather hierarchical. Specific
702 variants dominate expression in the parasite population in a reproducible order that
703 appears to be independent of the starting *VSG* [17,31,32,65,66]. In the *T. b. gambiense*
704 samples, we found two *VSGs* that met our detection threshold in multiple patients. In *T.*
705 *b. rhodesiense* samples, multiple patients shared a large proportion of expressed *VSGs*.
706 Given the large size of the genomic *VSG* repertoire, any overlap in expressed *VSG*
707 repertoire is likely indicative of a semi-predictable hierarchy of switching and preference
708 for the expression of certain *VSGs*.
709
710 Of the two shared *VSGs* we identified in the *T. b. gambiense* patients, one was
711 identified in two patients from the same village, while the other was found in two
712 patients from villages 40km apart. At this short distance, it is possible that the infecting
713 parasites were genetically similar. However, it would be interesting to investigate
714 whether preference for the expression of certain *VSGs* occurs even between parasites
715 isolated at greater distances. Indeed, past research has shown that the sensitivity of
716 serological tests for gHAT, which detect antibodies against the LiTat 1.3 VSG, vary
717 regionally, potentially due to differences in the underlying genomic or expressed *VSG*
718 repertoire in circulating strains [67,68].
719
720 Our data are consistent with the notion that there could be geographic variations in *T.*
721 *brucei VSG* repertoires. None of our assembled *T. b. gambiense VSGs* from patients in
722 the DR Congo shared significant N-terminal sequence similarity with those in the
723 genome of DAL972, a parasite isolate from Côte d'Ivoire. In contrast, the C-termini of
724 patient *VSGs* were well represented by similar sequences within the DAL972 reference.
725 Geographic variation has been observed in *var* gene repertoires of *Plasmodium*
726 *falciparum* [69] and the *VSG* repertoire of *Trypanosoma vivax*, another African
727 trypanosome [35]. A better understanding of such differences in *T. brucei*, if they exist,
728 could lead to development of more sensitive HAT diagnostics.
729
730 To better understand the VSG proteins expressed in natural infections, we developed
731 an HMM VSG typing pipeline that revealed an intriguing bias in *T. b. gambiense*
732 infection towards type B VSGs, which appears to be specific to *T. b. gambiense* patient
733 samples. Small sample sizes and important differences between each *T. brucei*
734 subspecies' dataset limit the conclusions that can be drawn. However, comparisons
735 between these sets suggest that the genomic *VSG* repertoire determines the
736 distribution of VSG N-terminal types expressed during *T. brucei* infection and may
737 account for the bias we have observed in *T. b. gambiense* patients. Thus, the *T. b.*
738 *gambiense VSG* repertoire may contain a larger proportion of type B VSGs than its
739 more virulent counterparts.
740
741 Another possibility we cannot rule out, however, is that the gHAT samples are biased
742 due to selection by the serological test used for diagnosis. Patients were screened for *T.*
743 *b. gambiense* infection using the CATT, a serological test that uses parasites
744 expressing VSG LiTat 1.3 as an antigen. LiTat 1.3 contains a type B2 N-terminal
745 domain [67,68]. Patients infected with parasites predominantly expressing type B VSGs

may be more likely to generate antibodies that cross-react with LiTat1.3, resulting in preferential detection of these cases. In contrast, *T.b. rhodesiense* can only be diagnosed microscopically, removing the potential to introduce bias through screening. It remains to be investigated whether samples from patients diagnosed using newer screening tests, which include the invariant surface glycoprotein ISG65 and the type A VSG LiTat 1.5 [29], would show similar bias towards the expression of type B VSGs.

Analysis of expressed VSG C-terminal domains in *T. b. gambiense* patients showed a bias towards C-terminal types 1 and 2. The diagnostic VSG LiTat1.3 contains a type 3 C-terminus, a C-terminal type underrepresented in the patient set. Therefore, it is unlikely that a bias in expressed C-terminal types is related to the screening method. Notably, the bias toward C-terminal types 1 and 2 was not reflected in the limited *VSG* repertoire of the DAL972 reference genome or the repertoire of the Lister 427 *T. b. brucei* reference genome. This finding could be related to the limited set of *VSG*s present in the DAL972 reference genome or reflect a true expression bias.

Could a bias towards certain VSG types, whether due to a difference in repertoire composition or expression preference, account for unique features of *T. b. gambiense* infection, including its chronicity and primarily anthroponotic nature [70]? While the genomic *VSG* repertoire has been analyzed extensively in laboratory strains, little is known about how differences in VSG proteins relate to parasite biology or whether there could be biological consequences to the expression of specific VSG N- or C-terminal types. Type A *var* genes in *Plasmodium falciparum* infection are associated with severe malaria [71–75], and similar mechanisms have been hypothesized to exist in *T. vivax* and *T. congolense* infections [33,35,76,77].

In *T. brucei,* several VSGs have evolved specific functions besides antigenic variation [77]. The first type B VSG structure was recently solved [78], revealing a unique *O*-linked carbohydrate in the VSG's N-terminal domain. This modification interfered with the generation of protective immunity in a mouse infection model; perhaps structural differences between each VSG type, including glycosylation patterns, could influence infection outcomes. Further research will be needed to determine whether the observed predominance of type B VSGs could influence the biology of *T. b. gambiense* infection.

Currently, it is unclear why this collection of gHAT patient isolates demonstrates a bias towards the expression of certain VSG types. More research will be needed to determine whether the *T. b. gambiense VSG* repertoire contains a unique distribution of VSG types, whether these parasites preferentially express certain VSG types, and whether this bias could have functional consequences. This study has shown, however, is that it is feasible to explore antigenic variation in natural infection. Moreover, although mouse models do reflect the general dynamics of antigenic variation in natural *T. brucei* infection, unique biology remains to be uncovered by studying this process in its natural context.

Acknowledgments

We are very grateful to the patients without whom this work would not have been possible. We thank George Cross and Danae Schulz for comments on the manuscript, and Mary Gebhardt for help with GIS. The Atlas of HAT is an initiative of the World Health Organization (WHO), jointly implemented with the Food and Agriculture Organization of the United Nations (FAO) in the framework of the Programme Against African Trypanosomiasis (PAAT). Field work and specimen collection in DR Congo were funded through the Wellcome Trust (study number 099310/Z/12/Z) awarded to the TrypanoGEN Consortium (www.trypanogen.net), members of H3Africa (h3africa.org). Sample work-up was supported by the Research Foundation Flanders (FWO grant 1501413N). Work by BW was supported by University of Nottingham/Wellcome Trust Institutional Strategic Support Fund award 204843/Z/16/Z. MRM and SS were supported by Office of the Director, NIH (DP5OD023065). JS is supported by NIH T32AI007417.

Supplement

Supplemental Table 1. Primer sequences.

Supplemental Table 2. gHAT patient distance matrix.

Supplemental Table 3. gHAT VSG expression data.

Supplemental Table 4. Tables comparing BLAST-tree, HMMscan, and network plot typing methods.

Supplemental Table 5. rHAT VSG expression data.

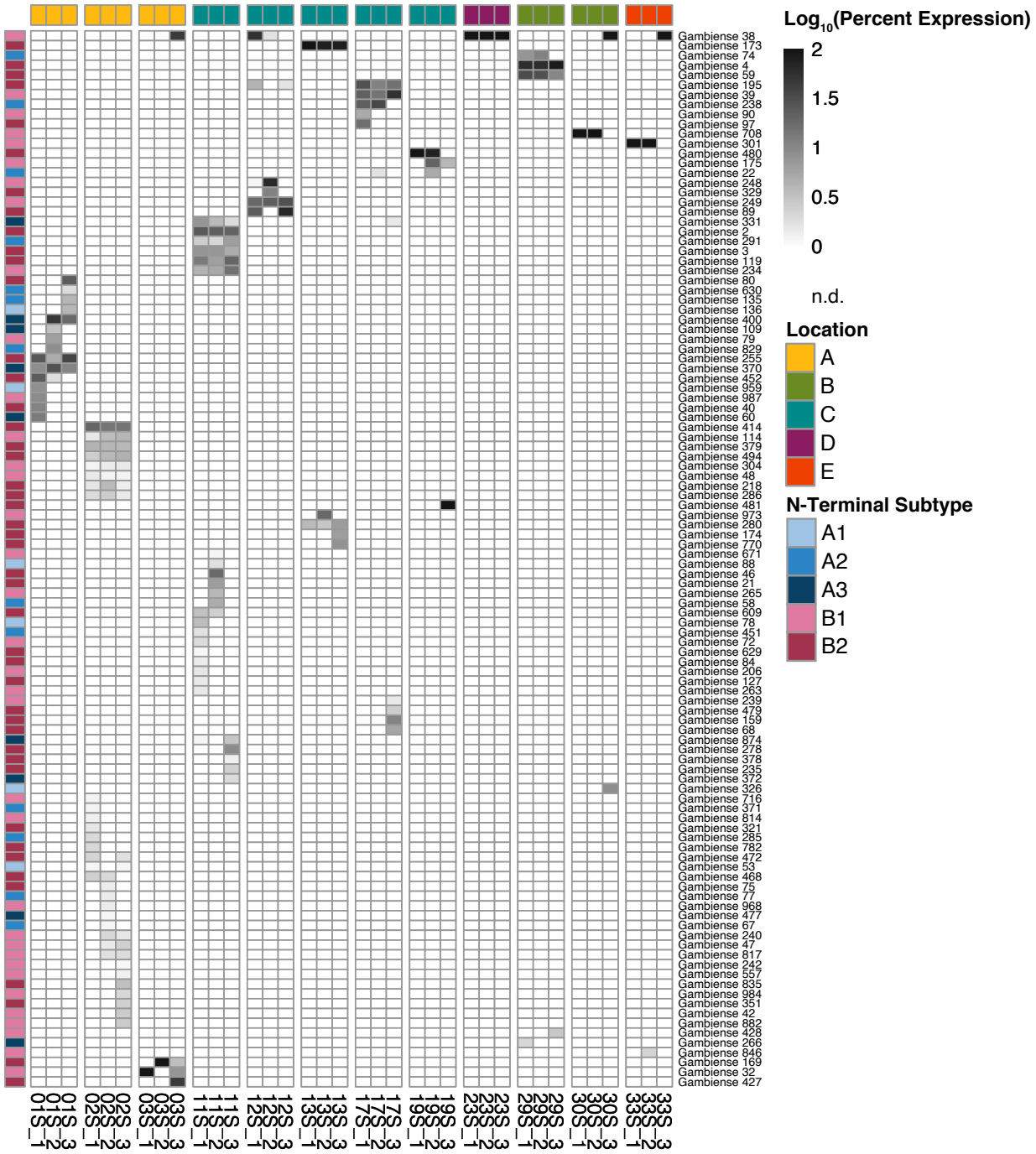

Supplemental Figure 1. Heatmap of all assembled *T.b. gambiense* patient VSGs. Greyscale shows $\log_{10}$ of the estimated percentage of the parasite population expressing each VSG. Variants expressed by less than 1% of parasites considered not detected (n.d.).

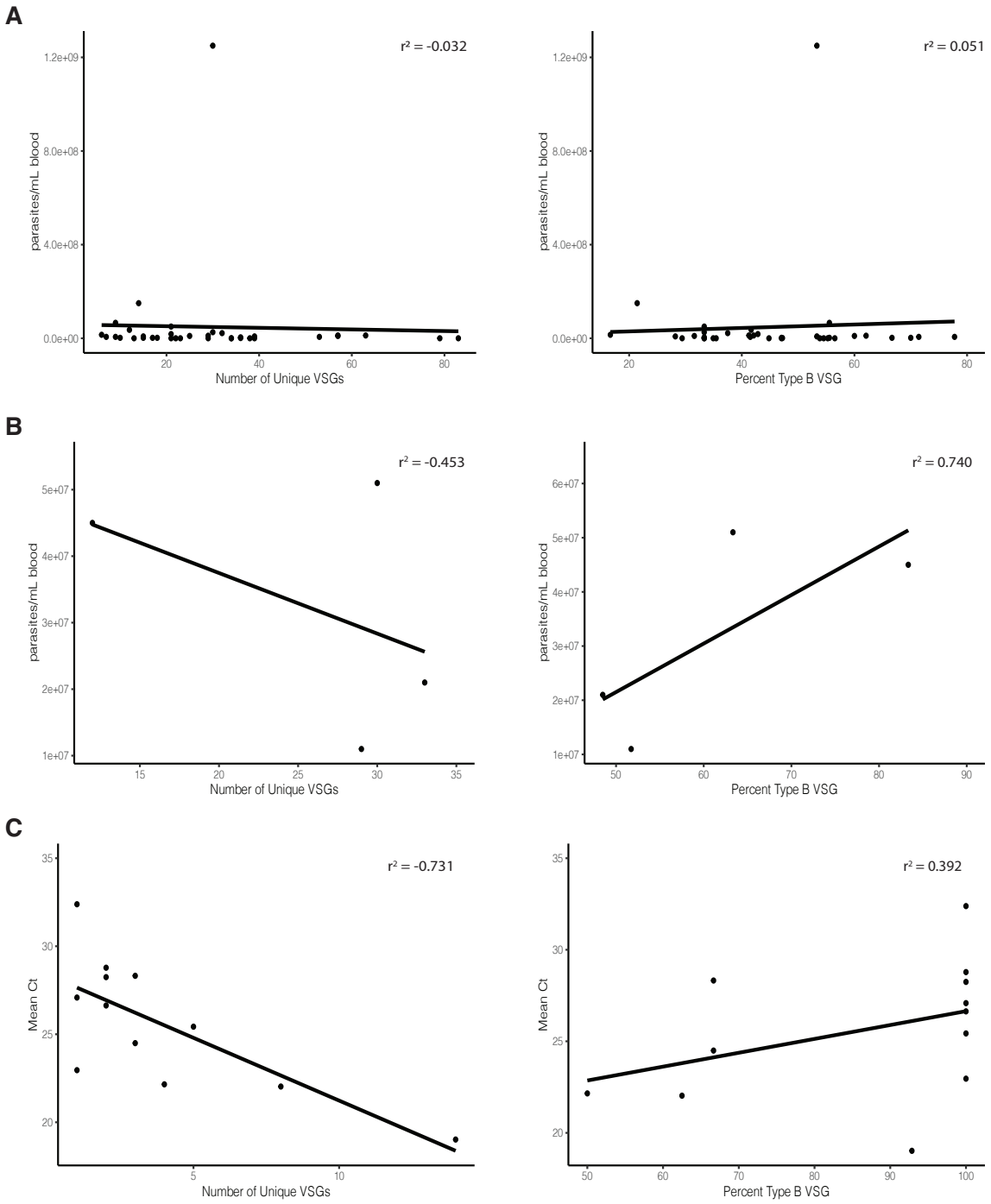

Supplemental Figure 2. Correlation between parasitemia and diversity and N-terminal type distribution. (A) Correlation plots for VSG diversity and percent of N-terminal domain type B for *T.b. brucei* infected mice from Mugnier et al. 2015. (B) Correlation plots for *T.b. rhodesiense* infected patients from Mulindwa et al. 2018. (C) Correlation plots for *T.b. gambiense* infected patients.

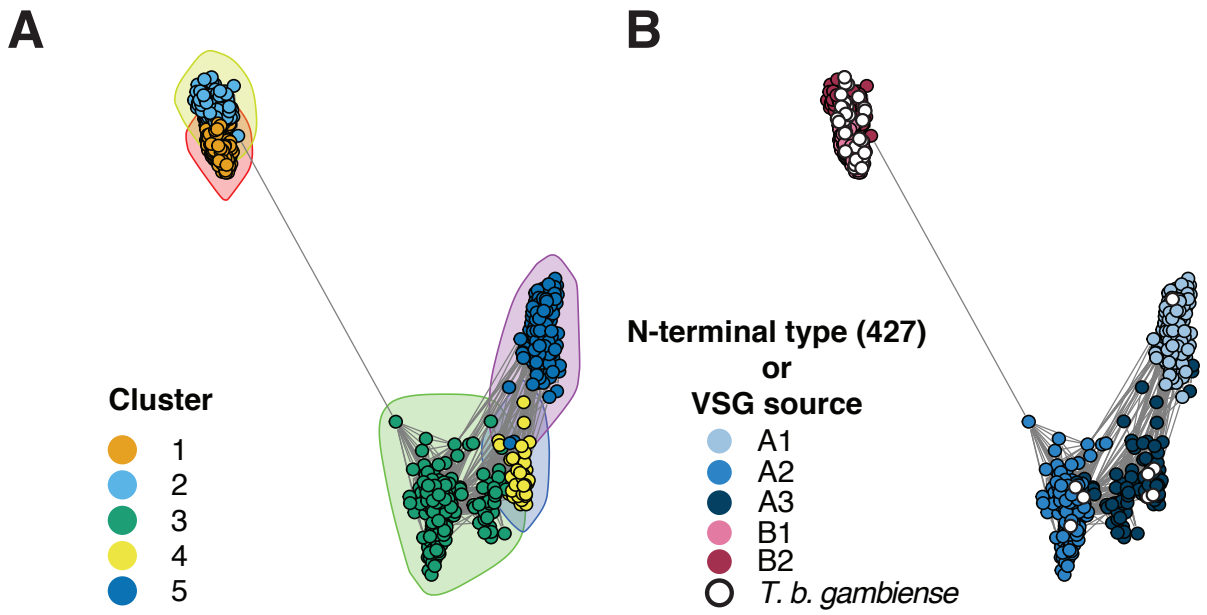

Supplemental Figure 3. (A) Network plot showing peptide sequence relatedness between N-terminal domains. Each point represents a VSG N-terminus. A link was drawn between points if the BLASTp e-value was less than 10^{-2}. Colors and shaded circles represent community assignments determined by the clustering algorithm. (B) The same graph as in (A), but points are manually colored by known N-terminal subtype from Cross et al. or by subspecies for VSGs identified in patients.

846
847 **Supplemental Figure 4. BLASTp-tree of all *T. b. gambiense VSGs.*** File attached.
848

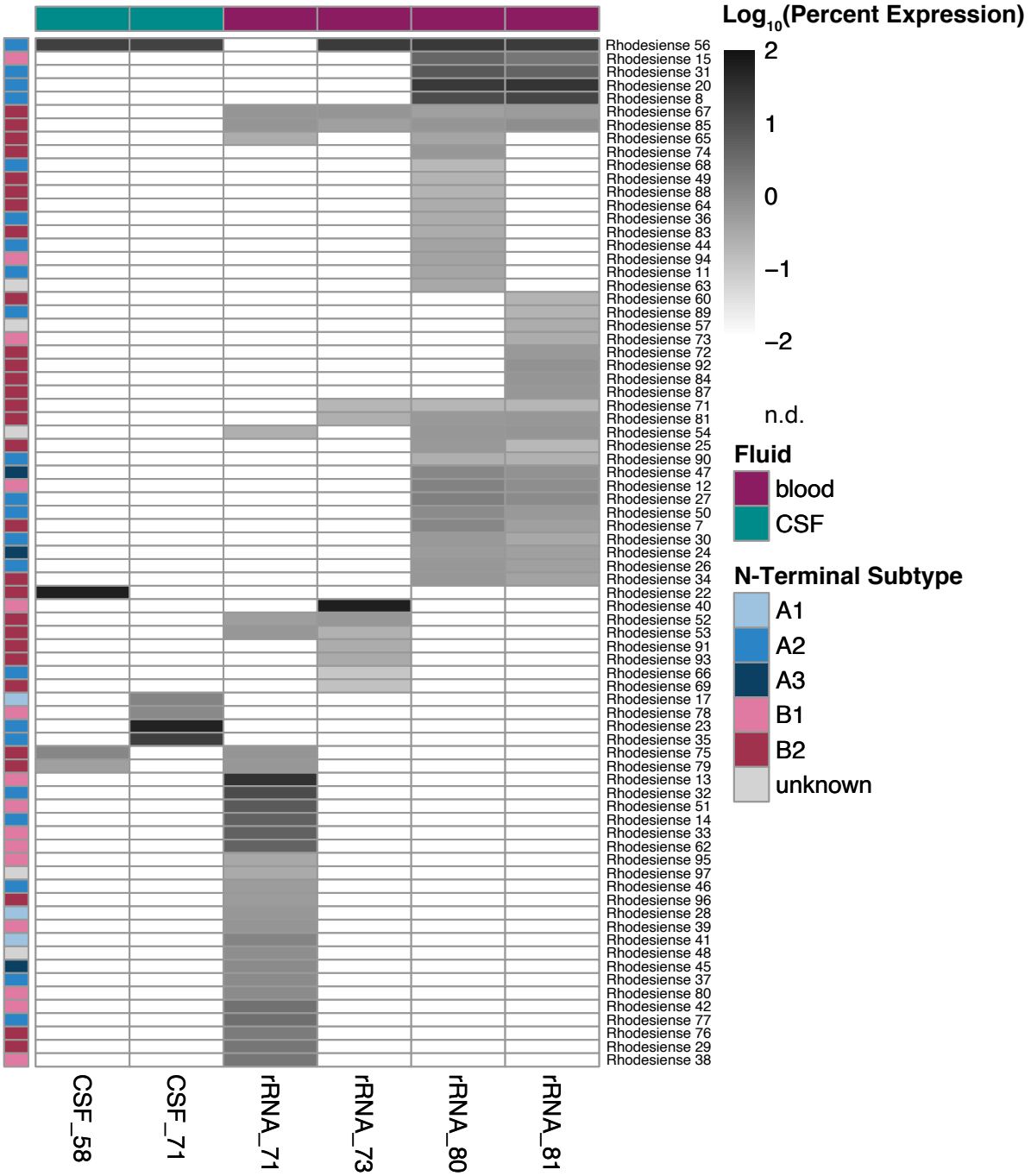

Supplemental Figure 5. Heatmap of all assembled *T. b. rhodesiense* patient VSGs. Greyscale shows $\log_{10}$ of the estimated percentage of the parasite population expressing each VSG. Variants expressed by less than 0.01% of parasites considered not detected (n.d.).

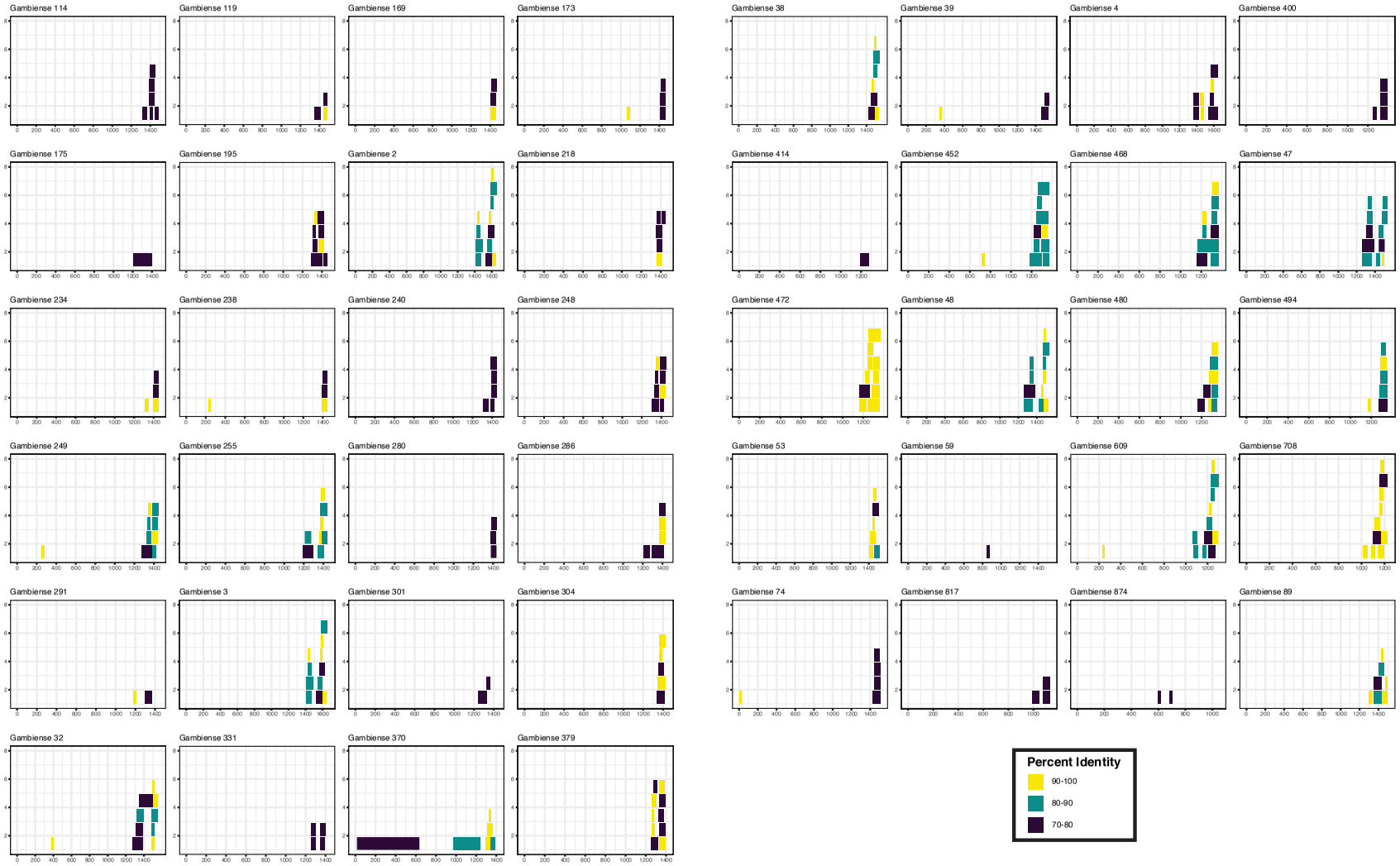
Gambiense 114
Gambiense 119
Gambiense 169
Gambiense 173
Gambiense 38
Gambiense 39
Gambiense 4
Gambiense 400
Gambiense 175
Gambiense 195
Gambiense 2
Gambiense 218
Gambiense 414
Gambiense 452
Gambiense 468
Gambiense 47
Gambiense 234
Gambiense 238
Gambiense 240
Gambiense 248
Gambiense 472
Gambiense 48
Gambiense 480
Gambiense 494
Gambiense 249
Gambiense 255
Gambiense 280
Gambiense 286
Gambiense 53
Gambiense 59
Gambiense 609
Gambiense 708
Gambiense 291
Gambiense 3
Gambiense 301
Gambiense 304
Gambiense 74
Gambiense 817
Gambiense 874
Gambiense 89
Gambiense 32
Gambiense 331
Gambiense 370
Gambiense 379
Percent Identity
90-100
80-90
70-80

Supplemental Figure 6. Ranges of all BLASTn hits with e-value < 0.1 for each assembled gHAT patient VSG against the TbgDAL972 whole genome reference. The full length of each patient VSG in base pairs is plotted as the X-axis of each plot facet. Bars color-coded by percent identity show each hit's alignment length and position within the query VSG. Alignments within the same query coordinates that hit multiple locations in the reference genome are stacked in bins. The maximum number of bins is plotted on the y-axis.

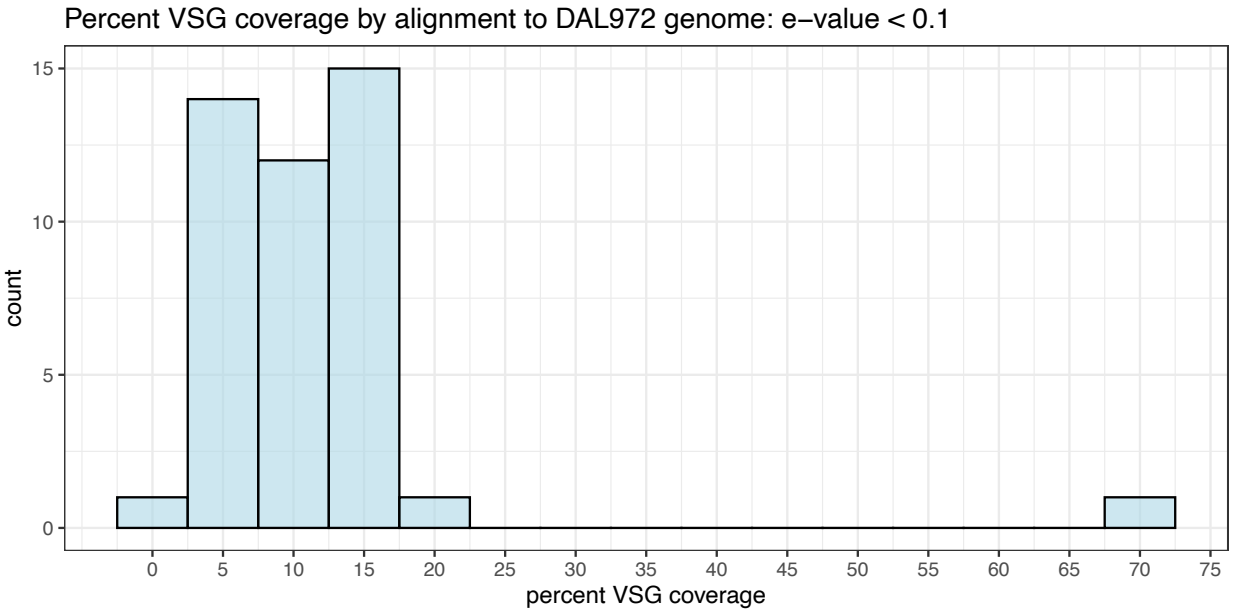

Supplemental Figure 7. Patient VSG representation within TbgDAL972. A histogram of the percentage of each patient VSG that was represented anywhere within the Tbg DAL972 genome by BLASTn with a threshold E-value < 0.1.

References

1. Romero-Meza G, Mugnier MR. Trypanosoma brucei. Trends in Parasitology. 2019. doi:10.1016/j.pt.2019.10.007
2. Büscher P, Cecchi G, Jamonneau V, Priotto G. Human African trypanosomiasis. www.thelancet.com. 2017;390. doi:10.1016/S0140-6736(17)31510-6
3. Franco JR, Cecchi G, Priotto G, Paone M, Diarra A, Grout L, et al. Monitoring the elimination of human African trypanosomiasis at continental and country level: Update to 2018. PLoS Negl Trop Dis. 2020;14: e0008261. doi:10.1371/JOURNAL.PNTD.0008261
4. Kennedy PGE, Rodgers J. Clinical and neuropathogenetic aspects of human African trypanosomiasis. Frontiers in Immunology. Frontiers Media S.A.; 2019. doi:10.3389/fimmu.2019.00039
5. Franco JR, Cecchi G, Priotto G, Paone M, Diarra A, Grout L, et al. Monitoring the elimination of human African trypanosomiasis at continental and country level: Update to 2018. PLoS Negl Trop Dis. 2020;14: e0008261. doi:10.1371/JOURNAL.PNTD.0008261
6. WHO. The Global Health Observatory. In: WHO [Internet]. World Health Organization; [cited 17 Aug 2021]. Available: https://www.who.int/data/gho/data/themes/topics/indicator-groups/indicator-group-details/GHO/human-african-trypanosomiasis
7. WHO. Ending the neglect to attain the sustainable development goals: a road map for neglected tropical diseases 2021–2030. Geneva; 2020.
8. Magez S, Caljon G, Tran T, Stijlemans B, Radwanska M. Current status of vaccination against African trypanosomiasis. Parasitology. 2010;137: 2017–2027.
9. Trindade S, Rijo-Ferreira F, Carvalho T, Pinto-Neves D, Guegan F, Aresta-Branco F, et al. Trypanosoma brucei Parasites Occupy and Functionally Adapt to the Adipose Tissue in Mice. Cell Host Microbe. 2016;19: 837–848. doi:10.1016/j.chom.2016.05.002
10. Pereira SS, Trindade S, De Niz M, Figueiredo LM. Tissue tropism in parasitic diseases. Open Biology. Royal Society Publishing; 2019. doi:10.1098/rsob.190036
11. Camara M, Soumah AM, Ilboudo H, Travaillé C, Clucas C, Cooper A, et al. Extravascular Dermal Trypanosomes in Suspected and Confirmed Cases of gambiense Human African Trypanosomiasis. Clin Infect Dis. 2021;73: 12–20. doi:10.1093/cid/ciaa897
12. Alfituri OA, Bradford BM, Paxton E, Morrison LJ, Mabbott NA. Influence of the Draining Lymph Nodes and Organized Lymphoid Tissue Microarchitecture on Susceptibility to Intradermal Trypanosoma brucei Infection. Front Immunol. 2020;11. doi:10.3389/fimmu.2020.01118
13. Marcello L, Barry JD. Analysis of the VSG gene silent archive in Trypanosoma brucei reveals that mosaic gene expression is prominent in antigenic variation and is favored by archive substructure. Genome Res. 2007;17: 1344–1352.
14. Berriman M, Ghedin E, Hertz-Fowler C, Blandin G, Renauld H, Bartholomeu DC, et al. The genome of the African trypanosome Trypanosoma brucei. Sci (New York, NY). 2005;309: 416–422.
15. Cross GAM, Kim H-S, Wickstead B. Capturing the variant surface glycoprotein

914 repertoire (the VSGnome) of Trypanosoma brucei Lister 427. Mol Biochem
915 Parasitol. 2014;195: 59–73. doi:10.1016/j.molbiopara.2014.06.004
916 16. Müller LSM, Cosentino RO, Förstner KU, Guizetti J, Wedel C, Kaplan N, et al.
917 Genome organization and DNA accessibility control antigenic variation in
918 trypanosomes. Nature. 2018;563: 121–125.
919 17. Hall JPJ, Wang H, Barry JD. Mosaic VSGs and the scale of Trypanosoma brucei
920 antigenic variation. Horn D, editor. PLoS Pathog. 2013;9: e1003502.
921 18. Jayaraman S, Harris C, Paxton E, Donachie A-M, Vaikkinen H, McCulloch R, et
922 al. Application of long read sequencing to determine expressed antigen diversity
923 in Trypanosoma brucei infections. Acosta-Serrano A, editor. PLoS Negl Trop Dis.
924 2019;13: e0007262. doi:10.1371/journal.pntd.0007262
925 19. Carrington M, Miller N, Blum M, Roditi I, Wiley D, Turner M. Variant specific
926 glycoprotein of Trypanosoma brucei consists of two domains each having an
927 independently conserved pattern of cysteine residues. J Mol Biol. 1991;221: 823–
928 835.
929 20. Hutchinson OC, Smith W, Jones NG, Chattopadhyay A, Welburn SC, Carrington
930 M. VSG structure: similar N-terminal domains can form functional VSGs with
931 different types of C-terminal domain. Mol Biochem Parasitol. 2003;130: 127–131.
932 21. Jones NG, Nietlispach D, Sharma R, Burke DF, Eyres I, Mues M, et al. Structure
933 of a glycosylphosphatidylinositol-anchored domain from a trypanosome variant
934 surface glycoprotein. J Biol Chem. 2008;283: 3584–3593.
935 22. Schwede A, Jones N, Engstler M, Carrington M. The VSG C-terminal domain is
936 inaccessible to antibodies on live trypanosomes. Mol Biochem Parasitol.
937 2011;175: 201–204.
938 23. Van Meirvenne N, Magnus E, Büscher P. Evaluation of variant specific
939 trypanolysis tests for serodiagnosis of human infections with Trypanosoma brucei
940 gambiense. Acta Trop. 1995;60: 189–199. doi:10.1016/0001-706X(95)00127-Z
941 24. Magnus E, Vervoort T, Van Meirvenne N. A card-agglutination test with stained
942 trypanosomes (C.A.T.T.) for the serological diagnosis of T. b. gambiense
943 trypanosomiasis. Ann Soc Belg Med Trop (1920). 1978;58: 169–176.
944 25. Dukes P, Gibson WC, Gashumba JK, Hudson KM, Bromidge TJ, Kaukus A, et al.
945 Absence of the LiTat 1.3 (CATT antigen) gene in Trypanosoma brucei gambiense
946 stocks from Cameroon. Acta Trop. 1992.
947 26. Enyaru JCK, Allingham R, Bromidge T, Kanmogne GD, Carasco JF. The isolation
948 and genetic heterogeneity of Trypanosoma brucei gambiense from north-west
949 Uganda. Acta Trop. 1993.
950 27. Bisser S, Lumbala C, Nguertoum E, Kande V, Flevaud L, Vatunga G, et al.
951 Sensitivity and Specificity of a Prototype Rapid Diagnostic Test for the Detection
952 of Trypanosoma brucei gambiense Infection: A Multi-centric Prospective Study.
953 Acosta-Serrano A, editor. PLoS Negl Trop Dis. 2016;10: e0004608.
954 doi:10.1371/journal.pntd.0004608
955 28. Büscher P, Mertens P, Leclipteux T, Gilleman Q, Jacquet D, Mumba-Ngoyi D, et
956 al. Sensitivity and specificity of HAT Sero-K-SeT, a rapid diagnostic test for
957 serodiagnosis of sleeping sickness caused by Trypanosoma brucei gambiense: A
958 case-control study. Lancet Glob Heal. 2014;2: e359–e363. doi:10.1016/S2214-
959 109X(14)70203-7

29. Lumbala C, Biéler S, Kayembe S, Makabuza J, Ongarello S, Ndung'u JM. Prospective evaluation of a rapid diagnostic test for Trypanosoma brucei gambiense infection developed using recombinant antigens. PLoS Negl Trop Dis. 2018;12: e0006386. doi:10.1371/JOURNAL.PNTD.0006386
30. Mugnier MR, Cross GAM, Papavasiliou FN. The in vivo dynamics of antigenic variation in Trypanosoma brucei. Science (80-). 2015;347: 1470–1473. doi:10.1126/science.aaa4502
31. Morrison LJ, Majiwa P, Read AF, Barry JD. Probabilistic order in antigenic variation of Trypanosoma brucei. Int J Parasitol. 2005;35: 961–972.
32. Lythgoe KA, Morrison LJ, Read AF, Barry JD. Parasite-intrinsic factors can explain ordered progression of trypanosome antigenic variation. Proc Natl Acad Sci U S A. 2007;104: 8095–8100.
33. Silva Pereira S, Heap J, Jones AR, Jackson AP. VAPPER: High-throughput variant antigen profiling in African trypanosomes of livestock. Gigascience. 2019;8. doi:10.1093/gigascience/giz091
34. Pereira SS, Casas-Sánchez A, Haines LR, Ogugo M, Absolomon K, Sanders M, et al. Variant antigen repertoires in Trypanosoma congolense populations and experimental infections can be profiled from deep sequence data using universal protein motifs. Genome Res. 2018;28: 1383–1394. doi:10.1101/gr.234146.118
35. Silva Pereira S, de Almeida Castilho Neto KJG, Duffy CW, Richards P, Noyes H, Ogugo M, et al. Variant antigen diversity in Trypanosoma vivax is not driven by recombination. Nat Commun. 2020;11: 844. doi:10.1038/s41467-020-14575-8
36. Hutchinson OC, Picozzi K, Jones NG, Mott H, Sharma R, Welburn SC, et al. Variant Surface Glycoprotein gene repertoires in Trypanosoma brucei have diverged to become strain-specific. BMC Genomics. 2007;8: 234. doi:10.1186/1471-2164-8-234
37. Ilboudo H, Noyes H, Mulindwa J, Kimuda MP, Koffi M, Kaboré JW, et al. Introducing the TrypanoGEN biobank: A valuable resource for the elimination of human African trypanosomiasis. PLoS Negl Trop Dis. 2017;11: e0005438. doi:10.1371/JOURNAL.PNTD.0005438
38. Camara M, Camara O, Ilboudo H, Sakande H, Kaboré J, N'Dri L, et al. Sleeping sickness diagnosis: use of buffy coats improves the sensitivity of the mini anion exchange centrifugation test. Trop Med Int Heal. 2010;15: 796–799. doi:10.1111/J.1365-3156.2010.02546.X
39. Simarro PP, Cecchi G, Paone M, Franco JR, Diarra A, Ruiz JA, et al. The Atlas of human African trypanosomiasis: A contribution to global mapping of neglected tropical diseases. Int J Health Geogr. 2010;9: 57. doi:10.1186/1476-072X-9-57
40. González-Andrade P, Camara M, Ilboudo H, Bucheton B, Jamonneau V, Deborggraeve S. Diagnosis of trypanosomatid infections: Targeting the spliced leader RNA. J Mol Diagnostics. 2014. doi:10.1016/j.jmoldx.2014.02.006
41. Brakenhoff RH, Schoenmakers JG, Lubsen NH. Chimeric cDNA clones: a novel PCR artifact. Nucleic Acids Res. 1991;19: 1949. doi:10.1093/NAR/19.8.1949
42. Meyerhans A, Vartanian J-P, Wain-Hobson S. DNA recombination during PCR. Nucleic Acids Res. 1990;18: 1687–1691. doi:10.1093/NAR/18.7.1687
43. Grabherr MG, Haas BJ, Yassour M, Levin JZ, Thompson DA, Amit I, et al. Full-length transcriptome assembly from RNA-Seq data without a reference genome.

1006 Nat Biotechnol. 2011;29: 644–652.
1007 44. Li W, Godzik A. Cd-hit: a fast program for clustering and comparing large sets of
1008 protein or nucleotide sequences. Bioinformatics. 2006;22: 1658–1659.
1009 45. Langmead B, Trapnell C, Pop M, Salzberg SL. Ultrafast and memory-efficient
1010 alignment of short DNA sequences to the human genome. Genome Biol. 2009;10:
1011 R25.
1012 46. Storvall H, Ramsköld D, Sandberg R. Efficient and comprehensive representation
1013 of uniqueness for next-generation sequencing by minimum unique length
1014 analyses. PLoS One. 2013;8: e53822.
1015 47. Conway JR, Lex A, Gehlenborg N. UpSetR: An R Package for the Visualization of
1016 Intersecting Sets and their Properties. doi:10.1101/120600
1017 48. Wickstead B, Gull K. Dyneins across eukaryotes: a comparative genomic
1018 analysis. Traffic. 2007;8: 1708–1721.
1019 49. Howe K, Bateman A, Durbin R. QuickTree: Building huge neighbour-joining trees
1020 of protein sequences. Bioinformatics. 2002;18: 1546–1547.
1021 doi:10.1093/bioinformatics/18.11.1546
1022 50. Paradis E, Schliep K. Ape 5.0: An environment for modern phylogenetics and
1023 evolutionary analyses in R. Bioinformatics. 2019;35: 526–528.
1024 doi:10.1093/bioinformatics/bty633
1025 51. Sievers F, Wilm A, Dineen D, Gibson TJ, Karplus K, Li W, et al. Fast, scalable
1026 generation of high-quality protein multiple sequence alignments using Clustal
1027 Omega. Mol Syst Biol. 2011;7: 539–539. doi:10.1038/msb.2011.75
1028 52. Eddy SR. Accelerated Profile HMM Searches. PLOS Comput Biol. 2011;7:
1029 e1002195. doi:10.1371/JOURNAL.PCBI.1002195
1030 53. Csárdi G, Nepusz T. The igraph software package for complex network research.
1031 54. Newman MEJ. Finding community structure in networks using the eigenvectors of
1032 matrices. Phys Rev E. 2006;74: 036104. doi:10.1103/PhysRevE.74.036104
1033 55. Lawrence M, Huber W, Pagès H, Aboyoun P, Carlson M, Gentleman R, et al.
1034 Software for Computing and Annotating Genomic Ranges. PLOS Comput Biol.
1035 2013;9: e1003118. doi:10.1371/JOURNAL.PCBI.1003118
1036 56. González-Andrade P, Camara M, Ilboudo H, Bucheton B, Jamonneau V,
1037 Deborggraeve S. Diagnosis of trypanosomatid infections: targeting the spliced
1038 leader RNA. J Mol Diagn. 2014;16: 400–404.
1039 57. Berberof M, Pérez-Morga D, Pays E. A receptor-like flagellar pocket glycoprotein
1040 specific to Trypanosoma brucei gambiense. Mol Biochem Parasitol. 2001;113:
1041 127–138.
1042 58. Weirather JL, Wilson ME, Donelson JE. Mapping of VSG similarities in
1043 Trypanosoma brucei. Mol Biochem Parasitol. 2012;181: 141–152.
1044 59. Mulindwa J, Leiss K, Ibberson D, Kamanyi Marucha K, Helbig C, Melo do
1045 Nascimento L, et al. Transcriptomes of Trypanosoma brucei rhodesiense from
1046 sleeping sickness patients, rodents and culture: Effects of strain, growth
1047 conditions and RNA preparation methods. Salavati R, editor. PLoS Negl Trop Dis.
1048 2018;12: e0006280.
1049 60. De Greef C, Hamers R. The serum resistance-associated (SRA) gene of
1050 Trypanosoma brucei rhodesiense encodes a variant surface glycoprotein-like
1051 protein. Mol Biochem Parasitol. 1994;68: 277–284.

1052 61. Jackson AP, Sanders M, Berry A, McQuillan J, Aslett MA, Quail MA, et al. The
1053 genome sequence of Trypanosoma brucei gambiense, causative agent of chronic
1054 human African Trypanosomiasis. PLoS Negl Trop Dis. 2010;4.
1055 doi:10.1371/journal.pntd.0000658
1056 62. Sistrom M, Evans B, Benoit J, Balmer O, Aksoy S, Caccone A. De Novo Genome
1057 Assembly Shows Genome Wide Similarity between Trypanosoma brucei brucei
1058 and Trypanosoma brucei rhodesiense. Louis EJ, editor. PLoS One. 2016;11:
1059 e0147660. doi:10.1371/journal.pone.0147660
1060 63. Sistrom M, Evans B, Bjornson R, Gibson W, Balmer O, Maser P, et al.
1061 Comparative genomics reveals multiple genetic backgrounds of human
1062 pathogenicity in the trypanosoma brucei complex. Genome Biol Evol. 2014;6:
1063 2811–2819. doi:10.1093/gbe/evu222
1064 64. Mugnier MR, Stebbins CE, Papavasiliou FN. Masters of Disguise: Antigenic
1065 Variation and the VSG Coat in Trypanosoma brucei. PLOS Pathog. 2016;12:
1066 e1005784. doi:10.1371/journal.ppat.1005784
1067 65. Aitcheson N, Talbot S, Shapiro J, Hughes K, Adkin C, Butt T, et al. VSG switching
1068 in Trypanosoma brucei: antigenic variation analysed using RNAi in the absence of
1069 immune selection. Mol Microbiol. 2006;57: 1608–1622. doi:10.1111/j.1365-
1070 2958.2005.04795.x.VSG
1071 66. Liu D, Albergante L, Newman TJ, Horn D. Faster growth with shorter antigens can
1072 explain a VSG hierarchy during African trypanosome infections: a feint attack by
1073 parasites. Sci Rep. 2018;8: 10922. doi:10.1038/s41598-018-29296-8
1074 67. Chappuis F, Loutan L, Simarro P, Lejon V, Büscher P. Options for field diagnosis
1075 of human african trypanosomiasis. Clin Microbiol Rev. 2005;18: 133–146.
1076 68. Truc P, Lejon V, Magnus E, Jamonneau V, Nangouma A, Verloo D, et al.
1077 Evaluation of the micro-CATT, CATT/Trypanosoma brucei gambiense, and
1078 LATEX/T b gambiense methods for serodiagnosis and surveillance of human
1079 African trypanosomiasis in West and Central Africa. Bull World Health Organ.
1080 2002;80: 882–886.
1081 69. Tonkin-Hill G, Ruybal-Pesántez S, Tiedje KE, Rougeron V, Duffy MF, Zakeri S, et
1082 al. Evolutionary analyses of the major variant surface antigen-encoding genes
1083 reveal population structure of Plasmodium falciparum within and between
1084 continents. PLOS Genet. 2021;17: e1009269.
1085 doi:10.1371/JOURNAL.PGEN.1009269
1086 70. Büscher P, Bart JM, Boelaert M, Bucheton B, Cecchi G, Chitnis N, et al. Do
1087 Cryptic Reservoirs Threaten Gambiense-Sleeping Sickness Elimination? Trends
1088 Parasitol. 2018;34: 197–207. doi:10.1016/J.PT.2017.11.008
1089 71. Kirchgatter K, del Portillo HA. Association of Severe Noncerebral Plasmodium
1090 falciparum Malaria in Brazil With Expressed PfEMP1 DBL1α Sequences Lacking
1091 Cysteine Residues. Mol Med 2002 81. 2002;8: 16–23. doi:10.1007/BF03401999
1092 72. Bull PC, Berriman M, Kyes S, Quail MA, Hall N, Kortok MM, et al. Plasmodium
1093 falciparum Variant Surface Antigen Expression Patterns during Malaria. PLOS
1094 Pathog. 2005;1: e26. doi:10.1371/JOURNAL.PPAT.0010026
1095 73. Abdi AI, Hodgson SH, Muthui MK, Kivisi CA, Kamuyu G, Kimani D, et al.
1096 Plasmodium falciparum malaria parasite var gene expression is modified by host
1097 antibodies: longitudinal evidence from controlled infections of Kenyan adults with

1098 varying natural exposure. BMC Infect Dis 2017 171. 2017;17: 1–11.
1099 doi:10.1186/S12879-017-2686-0
1100 74. Kyriacou HM, Stone GN, Challis RJ, Raza A, Lyke KE, Thera MA, et al.
1101 Differential var gene transcription in Plasmodium falciparum isolates from patients
1102 with cerebral malaria compared to hyperparasitaemia. Mol Biochem Parasitol.
1103 2006;150: 211–218. doi:10.1016/J.MOLBIOPARA.2006.08.005
1104 75. Duffy F, Bernabeu M, Babar PH, Kessler A, Wang CW, Vaz M, et al. Meta-
1105 analysis of plasmodium falciparum var signatures contributing to severe Malaria in
1106 African children and Indian adults. MBio. 2019;10. doi:10.1128/MBIO.00217-19
1107 76. Pereira SS, Casas-Sánchez A, Haines LR, Ogugo M, Absolomon K, Sanders M,
1108 et al. Variant antigen repertoires in Trypanosoma congolense populations and
1109 experimental infections can be profiled from deep sequence data using universal
1110 protein motifs. Genome Res. 2018;28: 1383. doi:10.1101/GR.234146.118
1111 77. Silva Pereira S, Jackson AP, Figueiredo LM. Evolution of the variant surface
1112 glycoprotein family in African trypanosomes. Trends Parasitol. 2021.
1113 doi:10.1016/J.PT.2021.07.012
1114 78. Pinger J, Nešić D, Ali L, Aresta-Branco F, Lilic M, Chowdhury S, et al. African
1115 trypanosomes evade immune clearance by O-glycosylation of the VSG surface
1116 coat. Nat Microbiol. 2018;19: 53.
1117
1118